Universidad Zaragoza

1542

Instituto de Nanociencia de Aragón

Final Master Project

REMOTE GUIDING OF NEURAL CELLS USING MAGNETIC NANOPARTICLES AND MAGNETIC FIELDS

Beatriz Romartínez Alonso

Directors: Gerardo F. Goya and M. Pilar Calatayud

ABSTRACT

Nerve regeneration, as a treatment of traumatic nerve injuries or degenerative diseases, has been pursued along the last decades, stimulating both basic and applied research. The strategies for nerve regeneration have been boosted recently by the consolidation of nanotechnology, allowing innovative approaches through physical or chemical guidance of axonal re-growth across the nerve gap after severe injury. As an example, many guidance therapies are based on nano-patterned scaffolds that serve as “nerve guidance channels” providing an effective conduit during the nerve regeneration process. These recent advances have provided new therapeutic possibilities as alternatives to established surgical techniques.

The present work has been developed within the framework of a novel, minimally invasive methodology for physical axon guidance based on the use of magnetic nanoparticles (MNPs) and magnetic fields (H). This strategy is based on the hypothesis that the neural cells can, under the application of an externally produced tensile force, guide the process of neurite outgrowth and axon elongation along the desired direction imposed by this force. The central goal of this work has been to demonstrate that magnetic nanoparticles (MNPs) can be used to generate these tensile forces under the effect of an external magnetic field gradient, and these forces can in turn provoke the orientation of neurites along the magnetic field direction.

The MNPs used for this purpose were polyethyleneimine-coated Fe_3O_4 nanoparticles (PEI-MNPs) with sizes of 25 ± 5 nm and good magnetic response. Neuron-like PC12 cell line was selected for in vitro experiments. PEI-MNPs showed low toxicity effects on PC12 cells. Nanoparticle uptake quantification was carried out via iron-thiocyanate complex colorimetric assay. The intracellular distribution of the PEI-MNPs was analyzed by TEM and dual-beam (FIB/SEM) techniques. These analyses revealed the coexistence of both fully incorporated PEI-MNPs and partially-internalized PEI-MNP-clusters crossing the cell membrane. The changes in morphology and cytoskeletal structure of cells exposed to PEI-MNPs were investigated using optical and confocal microscopy .When PEI-MNPs loaded PC12 cells were exposed to a static magnetic field (0.020 T), neurites outgrowth of PC12 cells was preferentially aligned to the direction of the magnetic force. An increment of the neurite length was also observed.

We demonstrated that the produced re-direction of the neurites has its origin in the magnetic force acting on the MNPs previously loaded into the neurites. Furthermore, an additional effect of the incorporated MNPs has been observed, i.e., that the MNPs can stimulate the neurite outgrowth process, opening the possibility of a two-fold therapy: remote orientation and stimulation of axonal growth. These results open the possibility of non-invasive, multifunctional therapies for nerve injury based on these MNPs and external magnetic fields.

Key words: Neurite outgrowth, Magnetic nanoparticles, Neuronal differentiation, Magnetic field, Regeneration.

RESUMEN

La regeneración del sistema nervioso, como tratamiento para las lesiones nerviosas traumáticas o enfermedades degenerativas, ha sido una idea perseguida a lo largo de décadas. El surgimiento de la nanotecnología ha permitido nuevas estrategias para la regeneración nerviosa, a través de enfoques innovadores basados en materiales nanoestructurados. Varias terapias de guiado neuronal se basan en estos 'andamios' nano-estructurados que sirven como "canales de guía de nervios " que proporcionan un conducto eficaz durante el proceso de regeneración del nervio.

El presente trabajo se ha desarrollado en el marco de una nueva metodología, mínimamente invasiva, para el guiado físico de neuritas y axones basada en el uso de nanopartículas magnéticas (NPM) y campos magnéticos aplicados remotamente. Esta estrategia se basa en la hipótesis de que las células neuronales pueden, bajo la aplicación de una fuerza de tracción producida y aplicada externamente, guiar el proceso de crecimiento de las neuritas y el alargamiento del axón a lo largo de la dirección impuesta por dichos campos magnéticos. El objetivo central de este trabajo ha sido demostrar que las nanopartículas magnéticas (NPMs) pueden utilizarse para generar estas fuerzas de tracción bajo el efecto de un gradiente de campo magnético externo, y estas fuerzas puede a su vez provocar la orientación de las neuritas a lo largo de la dirección del campo magnético.

Las NPMs utilizadas están compuestas por un núcleo magnético de Fe_3O_4 recubierto por polietilenimina (PEI-NPMs), con tamaños de 25 ± 5 nm. Células de la línea PC12 fueron seleccionadas como modelo neuronal para los experimentos in vitro. Las PEI-NPMs mostraron una baja toxicidad en células PC12, y su cuantificación se llevó a cabo a través de ensayos de absorción colorimétrica mediante un complejo de hierro-tiocianato. El estudio de la distribución intracelular de las NPMs mediante técnicas de doble haz (FIB / SEM) y TEM reveló la coexistencia de aglomerados de NPMs internalizados en el espacio intracelular, junto con otros aglomerados parcialmente internalizados, es decir, atravesando la membrana celular. Cuando las células PC12 cargadas con PEI-NPMs fueron expuestas a un campo magnético estático se observó que el crecimiento de las neuritas ocurría preferencialmente en la dirección de la fuerza magnética externa aplicada. Simultáneamente, se observó un incremento

estadísticamente significativo en la longitud promedio de las neuritas cuando éstas se encontraban cargadas con NPMs y sometidas al campo magnético externo.

Hemos demostrado que la orientación de los axones producida tiene su origen en la fuerza magnética que actúa sobre las NPMs previamente incorporadas a las neuritas. Por otra parte, se ha observado un efecto adicional de las NPMs incorporadas, específicamente que las NPMs pueden estimular el proceso de crecimiento de las neuritas, abriendo la posibilidad de una terapia bi-funcional: la orientación remota en conjunto con la estimulación del crecimiento axonal. Estos resultados abren la posibilidad de nuevas terapias multifuncionales no invasivas para lesiones nerviosas severas, mediante el uso de NPMs y de campos magnéticos externos.

Palabras clave: Crecimiento de neuritas, Nanopartículas magnéticas, Diferenciación neuronal, Campo magnético, Regeneración.

INDEX

INDEX OF FIGURES AND TABLES

I. INTRODUCTION

1. Nanotechnology and Nanomedicine

Nanotechnology can be defined as the design, characterization, production and application of structures, devices and systems by controlling shape and size at the nanometer-length scale; in other words nanotechnology is the engineering of functional systems at the molecular level or at < 100 nm range [1].

The medical application of nanotechnology is defined nanomedicine and is one of the fastest growth areas in nanotechnology. In recent decades, nanotechnology has become more widely used in diagnostic and therapeutic fields. Especially, multifunctional nanoparticle platforms hold great promise for use in therapeutic applications as a target probe or carrier of biomolecules, optical dyes, anti-target molecules, and bioactive drugs [2]. Many of the unique physical and biological properties of NPs are related to their small sizes (in the range of 5 to 100 nm) [3]. Furthermore, nanoscale materials and systems interact with biological systems at the molecular level so they can be used to manipulate and control behaviors and functions of biological systems.

2. Magnetic nanoparticles

Among nanometer-sized objects, nanoparticles (NPs) have proved to be useful as building blocks for the development of nano-biomaterials [3]. As intermediates between the molecular and the solid states, inorganic nanoparticles combine chemical accessibility in solution with physical properties of the bulk phase [2]. For any specific application in biomedical sciences, the selection of the NPs is often determined by the physical properties of the core material constituting them, as well as the chemical/biological characteristics of the functional coating.

Among these nanoscale materials investigated for biomedical use, magnetic nanoparticles (MNPs) have gained significant attention. MNPs are composed of magnetic materials such as iron, nickel, cobalt and their oxides like magnetite (Fe_3O_4), maghemite (γ-Fe_2O_3), cobalt ferrite (Fe_2CoO_4) or chromium di-oxide (CrO_2) [4, 5]. Specially, iron-oxide nanoparticles are the most employed for biomedical applications due to their smaller toxicity when compared to other magnetic materials such as cobalt and nickel [5]. Their application is possible due to their chemical stability and

biocompatibility [6, 7]. Therefore, MNPs are really interesting to bioscience due to their ability to respond to external, long range magnetic fields; this capacity have been exploited to manipulate NPs under external magnetic forces for targeting purposes, as well as for cell separation and labeling, drug delivery, magnetic resonance imaging (MRI) [6, 7], and heating at the nanometer scale in the field of magnetic hyperthermia [8].

Magnetic nanoparticles can be produced by a number of physical and chemical methods which determine the final properties of the product. These properties are defined by the nanoparticle shape and size, the size distribution and the surface chemistry of the resulting particles. The final magnetic properties of an ensemble of colloidal MNPs are strongly influenced by the degree of structural defects or impurities of the particle core and surface [5]. The most common methods described to synthesize iron-oxides nanoparticles in solution include co-precipitation, oxidative hydrolysis, microemulsions, and sol-gel reactions [5, 9].

Application of MNPs on biomedical areas requires the use of a colloidal ferrofluid, or magnetic colloids, which consist of a suspension of magnetic particles of nanometric sizes in a carrier liquid like water. MNPs tend to aggregate into large clusters, because of their large surface-to-volume ratio and dipole-dipole interaction [3]. The colloidal stabilization by the surface modification should provide biocompatible MNPs [10], and chemical functionality for the potential attachment of recognizable ligands or functional groups [10]. The general approach is the post addition of water-soluble ligands or polymers, such as polyethyleneimine (PEI) as stabilizing agent of MNPs [11, 12]. The efficacy of PEI-coated nanoparticles *in vivo* has been reported as considerably high and with potential for clinical uses [13].

Furthermore, the addition of bioactive molecules such as targeting moieties to the MNP surface is employed to increase their specificity toward cellular targets or to perform a specific function. Various biological molecules such as antibodies, growth factors, proteins, etc., may be bound to the polymer surfaces onto the nanoparticle by chemically coupling.

2.1.Physical properties: nanomagnetism and superparamagnetism

As the main interaction between magnetically loaded cells and the applied magnetic field is of a purely physical origin, it is important to star this section by briefly explaining the magnetic behavior of MNPs, in order to better understand their behavior under magnetic forces. MNPs have the ability to respond to an external magnetic field gradient that generates a magnetic force pulling the MNPs towards any desired target place. Therefore, these particles can be directed and concentrated within the target tissue by means of an external magnetic field.

The magnetism of a solid is originated from the contributions of the quantum properties of electrons constituting it. These electrons determine the magnetic behavior of the solid and the strength of the interaction between atoms in it. At macroscopic scales, these magnetic interactions between atoms, together with the crystalline structure of the solid, originate the magnetic response of materials (the response of a material when a magnetic field is applied on it). When the magnetic interactions are weak, the average magnetic moment will always be zero. However, for stronger magnetic interactions between the individual moments of the atoms, some materials exhibits magnetic order and the result is a nonzero macroscopic magnetization. These materials are known as ferromagnets. But despite this 'aligning interaction' a bulk piece of most ferromagnetic materials normally has a nearly zero macroscopic magnetic moment because the interior of the block is divided into magnetic domains (multidomain) (Figure 1). Within a single domain all magnetic moments remain parallel, but each domain is randomly oriented so that the net magnetic moment of the sample is nearly cancelled. When the volume of a small particle is reduced below a certain value, called critical domain size ($D_{Critical}$) the single-domain configuration is adopted (Figure 1). Within this single magnetic domain all the atomic magnetic moments will be magnetized along the same direction, adding up so they behave like a giant magnetic moment (superparamagnet). The value of critical size ($D_{Critical}$) below which a particle of a given material becomes single-domain is determined by intrinsic properties of that material (e.g., magnetic anisotropy, magnetic moment and exchange anisotropy), and also by the particle shape [15]. Although the actual D_C values depend on some preparation features, for magnetite the critical particle size has been accepted to be within the 80-100 nm range. Below these values the MNPs would be a single magnetic domain [16].

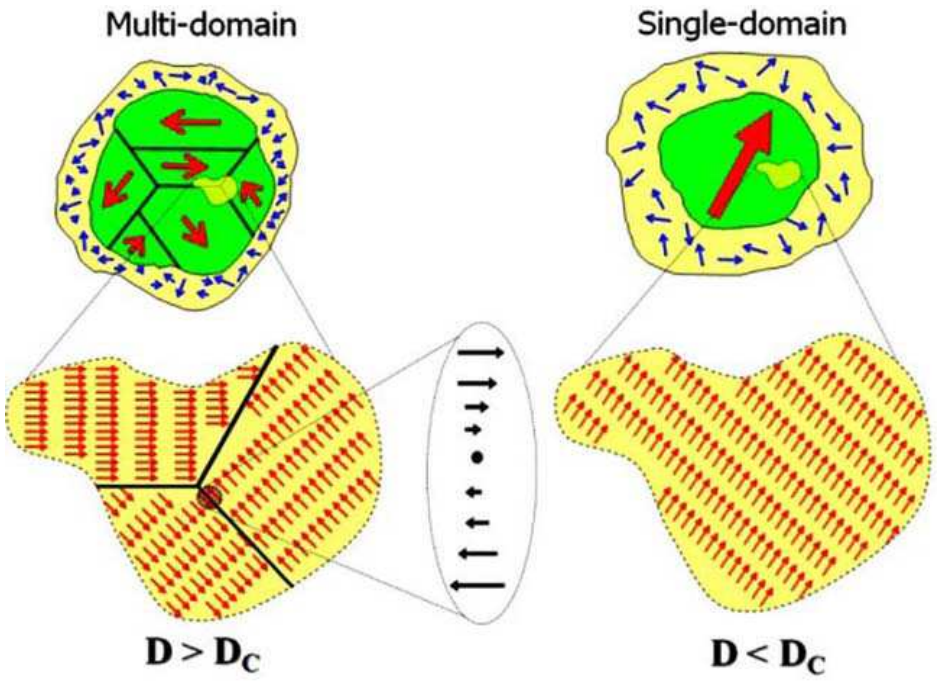

Figure 1. Differences between bulk ferromagnetic materials and particles with size bellow D_C. *Left: schematic view of magnetic domains in a multidomain ferromagnetic particle having size larger than the critical diameter $D>D_C$. For this particle the whole material breaks down into randomly oriented magnetic regions. Right: for $D<D_C$ the material becomes a single-domain particle. Adapted from [15].*

Superparamagnetism is characterized by not keeping magnetized after the action of magnetic field, offering advantage of reducing risk of particle aggregation [4]. Ferromagnetic NPs, whose size is bellow D_C, have a single magnetic domain and maintain one large magnetic moment (high ratio of induced magnetization –M- to the applied magnetic field –H). However at sufficiently high temperature (i.e. blocking temperature, T_B) thermal energy is sufficient to induce free rotation of the particle resulting in a loss of net magnetization in the absence of an external magnetic field [4]. Lack of remnant magnetization after removal of external fields enables the particles to maintain their colloidal stability and avoids aggregation making it feasible for their use in biomedical applications.

2.2.Iron oxide nanoparticles

Magnetic nanoparticles offers promising future perspectives for the treatment of injured neurons after accident or different type of disorders included neural degenerative disease. One such example is iron oxide nanoparticles. Iron oxide nanoparticles have magnetic properties and have attracted interests not only for *in vivo* tracking or imaging agents of neuronal cells [17, 18], but also for positioning cells in response to an external

magnetic field [19, 20]. Iron oxide nanoparticles can serve as a vehicle to deliver drugs to a target organ and/or tissue across the blood-brain barrier [21, 22].

Many studies have been conducted to evaluate the potential applications of iron oxide nanoparticles in the regeneration of neuronal functions; however, little is known about the influence of iron oxide nanoparticles on the intracellular or molecular level inside cells.

3. Magnetic nanoparticles for nerve regeneration

3.1. Biochemistry of neural cell differentiation and nerve regeneration

Nerve regeneration is a major issue in neuroscience in regard to the treatment of injured neurons after accident or degenerative diseases in order to recover nerve functionality. Extensive research in bioengineering is exploring innovative strategies to improve molecular and cellular therapies and to create physical or chemical guidance cues to direct axonal re-growth across the nerve lesion site.

Following injury, nerve regeneration is possible if the neuronal cell bodies are intact and the growing axons are provided with the proper microenvironment. Guidance cues that direct axonal re-growth along an appropriate spatial pathway are an important feature of the regeneration process because neurons have to reconnect with other neurons or with their correct target tissue via synapse formation.

The formation of neuronal processes and the neurite guide outgrowth is influenced by gradient of diffusible neurotrophic factors, cellular cues, substrate bound pathways, and surface topography. In vivo, glial cells provide a rich and supportive environment for neurite outgrowth through the release of neurotrophic factors, expression of cell surface ligands, and synthesis of extracellular matrix. Key among these are Schwann cells, glial cells of the peripheral nervous system whose presence in nerve grafts enhances the regeneration of both peripheral and central nerves.

Following a nerve transaction in the peripheral nervous system (PNS), the distal portion of the nerve begins to degenerate, in which the cytoskeleton and cell membrane of the disconnected axon begin to break down [23]. In response to axon transaction, the myelin sheath undergoes longitudinal segmentation. Schwann cells proliferate and

produce growth factors in response to denervation, cleaning up the debris of the degenerated region, and laying down tracks which will then retract when reinnervation occurs [24] (Figure 2). Nerve regeneration occurs at a rate of 2-4 mm/day after PNS injuries [25].

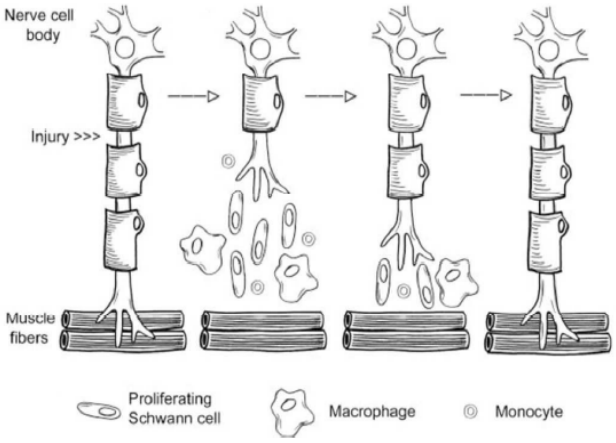

Figure 2. In the PNS, support cells aid neuronal regeneration. *Proliferating Schwann cells, macrophages and monocytes work together to remove myelin debris, release neurotrophins, and lead axons toward their synaptic targets, resulting in restores neuronal function.*

There are many types of neurotrophic molecules, but the most important and representative is nerve growth factor (NGF) that have a deep influence on cell developmental events, e.g., naturally occurring cell death, differentiation and process outgrowth. They have a distinct potential for the treatment of degenerative neurological condition by promoting neural regeneration [26]. NGF is vital to the development and regeneration of the nervous system, is expressed at low levels in healthy peripheral nerves but is up-regulated in the distal stump following injury [27]. Similarly, following spinal cord transaction, NGF accumulates in both the distal and proximal stumps [28]. At the cellular level, NGF, which acts through the high-affinity Trk A receptor [29], promotes survival, outgrowth, and branching in neurons, and inhibits cellular proliferation or mitosis.

3.2.Axon growth and guidance

The motile apparatus of neurons is the growth cone, a highly sensitive structure at the tip of growing axons. Axon guidance is responsible both for establishing neuronal

circuitry in the developing brain [30], and for the re-wiring of pathways that are damaged from injury or disease [31]. Growth cone behaviors such as advancing, retracting, turning and branching are regulated by dynamic reorganization of actin filaments and microtubules, which in turn are linked to the receptors for molecules called guidance cues, such as cell adhesion molecules (CAMs: integral membrane proteins mediating adhesion between growing axons and eliciting intracellular signaling within the growth cone), developmental morphogens, growth factors (NGF), neurotransmitters, etc. Growth cones integrate complex cues which vary in both time and space, and how all of these pieces fit together is less understood. Most axon guidance receptors activate signal transduction cascades that ultimately lead to reorganization of the cytoskeleton and adhesive properties of the growth cone, which together underlie the motility of neural cells. Recent progress indicates that focal adhesions may function as the biomolecular integration point of growth cone signaling and response [32].

Focal adhesions (FAs) are integrin-based adhesions whose stability determines the initiation and extension of neurites in differentiating neurons [33, 34]. Integrins comprise a large family of cell adhesion transmembrane proteins that mediate interactions between the extracellular environment and the cytoplasm. Integrins regulate many aspects of cell behavior including cell death, proliferation, migration, and differentiation and are the predominant molecular transducers of force [35].

Neurites are long cellular protrusions off the cell body that emerge when differentiation starts. The emerging neurites grow and find their way toward specific targets in the body following the guidance cues, so, eventually, they are responsible of the migration and polarization of the differentiating neurons. The maturation of FAs likely plays an essential role in sensing local substrate information and coordinating the morphometric changes that characterize the establishment of cell polarity during neuronal differentiation [34, 36].

Goals of neural tissue engineering for nerve injury include trying to find a way to guide axons with cues to achieve directed neuronal growth. Engineered MNPs opens their potential for both positioning and guiding neural cells in response to an external magnetic field [20, 37]. In particular, the approach of using MNPs as an alternative to

surgical nerve grafting for the treatment of severe peripheral nerve injuries is one of the most appealing applications.

3.3.Effects of MNPs in nerve regeneration

Kim and collaborators reported in 2011 that iron oxide nanoparticles can enhance neurite outgrowth [37]. Neural cells exposed to both iron oxide nanoparticles and nerve growth factor (NGF) synergistically increased the efficiency of neurite outgrowth [37]. They proposed that their results are due to the activation of cell adhesion molecules that are associated with cell-matrix interactions through iron. Iron oxide nanoparticles upregulate the expression of a neural specific marker and a cell adhesion protein (integrin). Thus, they hypothesized that iron oxide nanoparticles can affect cell-substrate interaction and regulate cell behaviors.

These results are in agreement with the information presented in the previous part that expose that cell adhesion molecules regulate cell differentiation, proliferation, migration and survival by interacting with extracellular molecules, such as integrin which is one of the adhesion molecules. If iron oxide nanoparticles stimulate focal adhesion of neurites, neurites outgrowth would be improved.

Recently, it has been discovered that iron oxide nanoparticles can attenuate oxidative stress in a neutral pH environment *in vitro* and, in combination with an external electromagnetic field, they can also facilitate axon regeneration [38]. The primary injury caused by nerve transaction is generally followed by secondary damage that results in a number of morphological, physiological, and biochemical changes, including inflammation, disruption of neurological pathways, demyelination, and cell death at the site of the lesion [38]. Cyst formation and robust infiltration of fibroblast result in formation of fibrous scar tissue that creates a physical barrier, preventing any severed axons or collateral branches of uninjured axons from growing past the area of the lesion. The free radical scavenging properties of iron oxide NPs can reduce the formation of fibrous scar tissue or secondary damage which is positively correlated with functional recovery [38].

Iron oxide nanoparticles have the potential to promote regeneration and axon growth in presence of an external magnetic field, thereby helping to bridge the gap at the injury site [39]. Retention and accumulation of iron oxide NPs in cells can be enhanced by an

external magnetic field , providing mechanical tensile forces that may cause axonal sprouting [39]. An external magnetic field can magnetize nanoparticles such that their beneficial effects can be focused to the site of injury. An external magnetic field also can noninvasively create intense rapid electric fields in deep underlying structures. If the current created is of sufficient amplitude and duration such that depolarization occurs, neural tissue is stimulated. Magnetic stimulation provides a microenvironment conducive to neural repair by stimulating release of neurotrophic factors that promote migration of glial cells to the site of the lesion and decrease apoptosis after neuronal injury [40]. Thus, combination of these effects (iron oxide NPs and magnetic fields) may reduce the secondary damage and facilitate of axonal and neuronal regeneration, by reducing the lesion volume and due to the neuroprotective effect against oxidative stress [38].

3.4.Effects of a magnetic field in nerve regeneration and remote guidance

It is well documented that cells can respond to the mechanical properties of their environments, including stiffness [41], shear flow [42], and mechanical stretch [41]. The process of mechanotransduction, which is how cells convert physical force into a biochemical signal, has been shown to occur through integrins, as well as through mechanosensitive ion channels [43] and G-protein coupled receptors [44]. In addition, focal adhesion sites have the ability to strengthen when forces are applied to them. So, mechanosensing has been hypothesized to play a role in cellular migration. It has been suggested that mechanical forces on cellular membranes are capable of rearranging membrane components such as integrin complexes. Focal adhesion structures are capable of changing localization, composition and cellular behavior in response to mechanical stimuli, and are hypothesized to be the functional linker between the extracellular matrix to the intracellular cytoskeleton [45].

The application of magnetic fields can be used to modulate the orientation and direction of neurite formation in cultured human neuronal cells [46]. In presence of a static magnetic field, neurites grow in a specific direction due to the application of magnetic fields change the co-localization of microtubule and actin filament in culture cells, that is, the subcellular polarity of the microtubule-actin interaction is induced by an external magnetic field [46].

There is a force F generated on the attached MNPs when a magnetic particle with magnetic moment is placed in a non-uniform magnetic field. The force F creates a mechanical tension on the axon which stimulates nerve regeneration in the direction imposed by the magnetic field. Thus, magnetic nanoparticles would influence or stimulate the focal adhesion of the growth cone in the axon by mechanical stretch, in the direction imposed by the external magnetic field, and would act as a guidance cue to direct the neurite outgrowth (Figure 3).

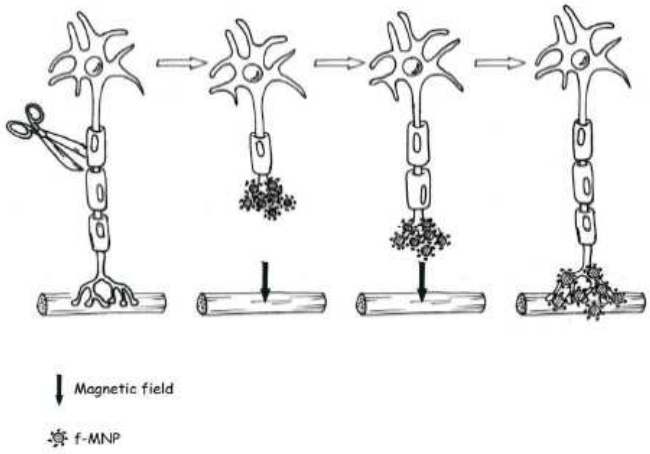

Figure 3. Nerve regeneration mediated by MNPs. *MNPs bind the injured nerve, a magnetic field is thus applied in the direction of the nerve regeneration. MNPs create a mechanical tension which stimulates nerve regeneration in a direction imposed by the magnetic field.*

The physical guidance should direct more efficiently the regeneration of the injured nerve from the proximal to the distal stump. Additionally, MNP binding to the neuronal cells can be enhanced with biological molecules, e.g. neural binders and neurotrophic factors (NGF). The functionalization of MNPs with specific cellular ligands, able to bind selectively to the surface receptors of the neurons, could increase the specificity as well as the efficiency of the process.

II. OBJECTIVES

The aim of this research project has been to investigate a novel approach to stimulate nerve regeneration based on the use of magnetic nanoparticles (MNPs), which can be manipulated by external magnetic fields. This 'action at distance', combined with the intrinsic penetrability of magnetic fields through human tissues, have been used to induce a mechanical force at neuron level in order to stimulate and initiate axon re-growth in the desired direction.

In this work, I present a study that investigates the effects of iron oxide nanoparticles on the neurite outgrowth during differentiation in the presence of an external magnetic field.

The present work had the following objectives:

Didactic Objectives

- To develop an experimental project with independence and originality.
- To apply the theoretical knowledge to the interpretation and analysis of the experimental data.
- To improve skill at oral and written communication, circulating the results and, interaction with colleagues and professionals from other disciplines.

Experimental Objectives

- Cell culture and measurement of magnetic nanoparticles uptake by a neural cell lineage (PC12).
- To design experimental strategies handling biocompatible magnetic nanoparticles, cell cultures and magnetic fields, in the field of neural regeneration.
- Characterization of PC12 cells after the treatment with magnetic nanoparticles by electronic microscopies (TEM and Dual Beam SEM-FIB analysis) and confocal optical microscopy.

III. MATERIALS AND METHODS

1. Synthesis of PEI coated Fe_3O_4 nanoparticles (PEI-MNPs) and fluorescent PEI-Fe_3O_4 nanoparticles.

The PEI-MNPs used in these experiments were synthesized and characterized as described elsewhere [14]. Briefly, the magnetite nanoparticles were synthesized by an oxidative hydrolysis method [7]. In a typical synthesis, a mixture of KNO_3 and NaOH was dissolved in distilled water in a three-necked flask bubbled with N_2. A H_2SO_4 solution containing $FeSO_4 \cdot 7\ H_2O$ and polyethyleneimine (PEI 25 kDa, Figure. 4) (previously flowed with N_2 for 2 hrs) was added dropwise under constant stirring. After precipitation a nitrogen flow was passed while temperature was maintained at 90º C for 24 h, and finally cooled to room temperature with an ice bath. The resulting black product was separated by magnetic decantation and washed several times with Q-water to remove all the impurities and get physiological pH.

Fluorescent labeling of PEI-Fe_3O_4 nanoparticles (f-PEI-MNPs)

The free amine groups of PEI-MNPs were tagged with the fluorescent dye alexa 488 (Figure 4). 2.5 mg of PEI-MNPs were suspended in 1 ml of 0.1 M sodium carbonate-bicarbonate buffer at pH 9.5 to ensure the deprotonation of amine groups on the PEI polymer coating. Alexa 488 solution (1 mg/ml DMSO: 20 µl) was then added to the PEI-MNPs suspension and the reaction mixture suspension was covered with aluminum foil and rotated (using a Rotator) at room temperature for 3 hours. The Alexa 488-labelled PEI-MNPs were finally washed with deionized H_2O until no further fluorescence was observed in the supernatant. The sample is denoted as f-PEI-MNPs.

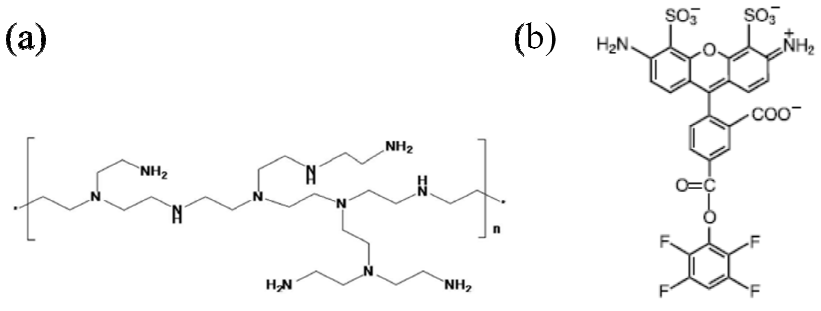

***Figure 4**. (a) Chemical structure of polyethyleneimine (PEI 25 kDa). (b) Alexa Fluor® 488 carboxylic acid, TFP ester, bis (triethylammonium salt); (MW ~885).*

2. Physicochemical characterization of magnetic nanoparticles

The obtained MNPs were characterized in terms of external morphology, microstructure, size distribution and magnetic properties.

2.1.Transmission electron microscopy (TEM)

MNPs average size, distribution and morphology were analyzed by transmission electron microscopy (TEM) using a FEI Tecnai T20 microscope and operating at 200 keV. TEM samples were prepared by placing one drop of a dilute suspension of magnetite nanoparticles in water on a carbon-coated copper grid and allowing the solvent to evaporate at room temperature. The average particle size (DTEM) and distribution were evaluated by measuring the largest internal dimension of 200 particles.

2.2.Zeta potential

The zeta potential and isoelectric point were evaluated at room temperature on a photo correlation spectrometer (PCS) Brookhaven 90 plus from a dilute suspension of the sample in water in a zeta-potential cuvette with 0.01 M concentration of KCl.

2.3.Magnetic characterization

The magnetic characterization was carried out using a SQUID Magnetometer (Quantum Design MPMS-XL). Zero-field-cooled (ZFC) and field-cooled (FC) curves were measured between 5 K and 250 K, with cooling field H_{FC} = 100 Oe. For the ZFC curves, the samples were first cooled from room temperature in zero applied field to the basal temperature (10 K). Then a field was applied and the variation of magnetization (M) was measured with increasing temperature up to T = 250 K. After the last point was measured, the FC curve was taken by cooling the sample keeping the same field; then the M vs. T data was measured increasing temperatures. Low-temperature hysteresis loops (10-250 K) were obtained in applied fields up to 5 T.

3. *In-vitro* experiments

3.1. PC12 Cell culture

Rat pheochromocytoma PC12 cells obtained from American Type Culture Collection (ATCC) were cultured in Dulbecco's modified Eagle's medium (DMEN; Lonza, Verviers, Belgium) with 10 % horse serum, 5 % fetal bovine serum, 100 IU/mL penicillin, 100 µg/mL streptomycin and 2 mM L-glutamine in T-25 flasks (growth medium). Cells were maintained at 37 ºC in a saturated humidity atmosphere of 95 % air and 5 % CO_2. Before cell seeding, well plates were coated with poly-l-lysine (PLL) (Sigma 81339). For cell differentiation, nerve growth factor (NGF, 80 ng/ml) was added into serum-reduced media (2% FBS).

In-vitro experiments were designed at 10 µg/mL of PEI-MNPs. After the incubation time (24 h) the cells were washed and the modified-DMEM was replaced with ordinary DMEM**.** Control experiments were performed with growth medium without nanoparticles. When cultured for 5 days with or without magnets, the cell morphology and length and orientation of neurites were investigated.

3.2. Quantification of uploaded PEI-MNPs in PC12 cells

Iron oxide nanoparticles content into PC12 cells was quantified by thiocyanate colorimetric assay. Cells were seeded (500,000 cells/mL) in 6-well dishes (1 mL growth medium and 500,000 cells/well) and treated with PEI-MNPs (5-50 µg/mL). After 24 hours of incubation, cells were isolated and lysed in HCl 6M-HNO_3 (65 %) for 2 h to dissolve all the components including nanoparticles. Samples were diluted with HCl 6 M and filtered. The iron content was determined by adding potassium thiocyanate to the Fe^{3+} solutions in order to form the iron-thiocyanate complex, which has strong absorbance at 478 nm wavelength. The iron concentration was determined by comparing the sample absorbance to a calibration curve.

3.3. SEM and Dual beam (FIB/SEM) analysis of PC12 cells incubated with PEI-MNPs

To assess the cellular distribution of PEI-MNPs, scanning electron microscopy (SEM INSPECT F50, FEI Company) and dual-beam FIB/SEM (Nova 200 NanoLa, FEI Company) analysis images were taken in conditioned samples of PC12 neuron-like cells. SEM images were taken at 5 and 30 kV with a FEG column and a combined Ga-based 30 kV (10 pA) ion beam was used to cross-sectioning single cells. These investigations were completed by energy-dispersive X-Ray spectroscopy (EDX) for chemical analysis. The preparation of the cells was made by seeding cells onto sterile glass cover slips (12 mm Ø) inside 35 mm dishes (Ibidi Petri dishes, cod. 80156, Ibidi, Germany) at a density of 25,000 cells/well in 800 µL of culture medium for 24 hours. After that, the growth medium was removed and replaced with medium containing 10 µg/mL MNPs. Then, the cells were induced to differentiate with NGF (80 ng/mL) and incubated for 4 days. After differentiation the cells were washed with PBS and fixed with 2 % glutaraldehyde solution for 2 hours at 4 ºC and washed again with PBS. Next, cells were incubated with 2 % osmium tetroxide and 2.5 % potassium ferrocyanide $K_3[Fe(CN)_6]$ for 1 hour at room temperature and darkness. Subsequently and after washing with 0.1 M phosphate-buffered saline (PBS), the cells were dehydrated via immersion in increasing concentrations of methanol 30 %, 50 %, 70 % and 90 % followed by further dehydration with anhydrous MeOH. After drying the samples were sputtered with 30 nm of gold.

3.4. Immunocytochemistry assay in PC12 cells: actin and tubulin fluorescent staining

The preparation of cells for immunocytochemistry was made by seeding cells onto sterile 35 mm dishes (Ibidi Petri dishes, cod. 80156, Ibidi, Germany) previously treated with PLL, at concentration of 25,000 cells/well in 800 µL of culture medium and incubated overnight to allow cell adhesion. f-PEI-MNPs (Alexa Fluor® 488) were added at a concentration of 10 µg/mL and incubated 24 h, after that, cells were cultivated in differentiation medium for 4 days. The PC12 cells were fluorescent stained for tubulin and actin, separately.

Phalloidin staining

For actin staining, the PC12 cells were rinsed briefly with PBS and fixed with 3 % paraformaldehyde for 15 minutes. After washing, cells were blocked with 5 % bovine serum albumin in PBS for 15 min. After washing again with PBS, the cells were permeabilized by the addition of 1 % bovine serum albumin and 0.1 % saponin in PBS (permeabilization solution) and incubated for 1 hour. To visualize actin, samples were incubated with phalloidin-alexa fluoride® 546 (1:200) in BSA/saponin/PBS for 1 hour and finally, were rinsed again and put together in cover slips (20 mm Ø) with Mowiol/DAPI (1000:1). DAPI (4,6-diamidino-2-phenylindole 5 mg/mL) was used to visualize nuclei. All steps were performed at darkness and at room temperature.

Tubulin staining

The PC12 cells were rinsed with PBS and fixed with cold methanol for 15 min at -4 ºC. After washing, cells were blocked with 5 % bovine serum albumin in PBS for 15 min at room temperature. In this case, the permeabilization and the tubulin labeling were made simultaneously. After washing again with PBS, mouse monoclonal anti-neuronal class III beta tubulin (β-III-tubulin) primary antibody diluted 1:400 in permeabilization solution (BSA/saponin/PBS) was added to the samples in order to label tubulin and incubated for 1 hour at room temperature. Then, samples were rinsed in permeabilization solution, incubated for 1 h at room temperature with Alexa fluor® 633-conjugated goat anti-mouse secondary antibody diluted 1:500 in permeabilization buffer and lastly, assembled with Mowiol/DAPI in cover slips (20 mm Ø).

Finally, all the assembled samples were dried and analyzed by confocal microscopy.

4. Neurites orientation and outgrowth: experimental set-up

PC12 cells (800 cells/cm^2) were seeded in T-25 flasks previously treated with poly-L-lysine coating (PLL, 10 µg/mL) which gives the cover glass an effective positive charge that increases cellular adhesion. After 24 hours, the cells were incubated with 10 µg/mL of PEI- MNPs overnight. The next day, the medium-containing PEI-MNPs was replaced

with differentiation medium (NGF 80 ng/mL) to induce neural differentiation and the culture was placed into a magnetic field applicator (Figure 5). This home-made applicator produced an external magnetic field created by two parallel Nd-Fe-B (neodymium-iron-boron) magnets of 15x20x5 mm^3 separated by a thin constant distance of 2 mm. The resulting magnetic field within this 2 mm-gap was simulated by a finite element simulation program, to get the expected values of magnetic induction B and also the magnetic field gradient ∇B since both parameters determine the resulting magnetic forces on the MNPs. The results (Figure 5) of the numeric simulation showed that the value of B was expected to be B = 0.19 - 0.20 T within the area of analysis. The permanent magnets faced each other with opposite poles and the distance between them was 2 mm. The configuration is shown in Figure 5.

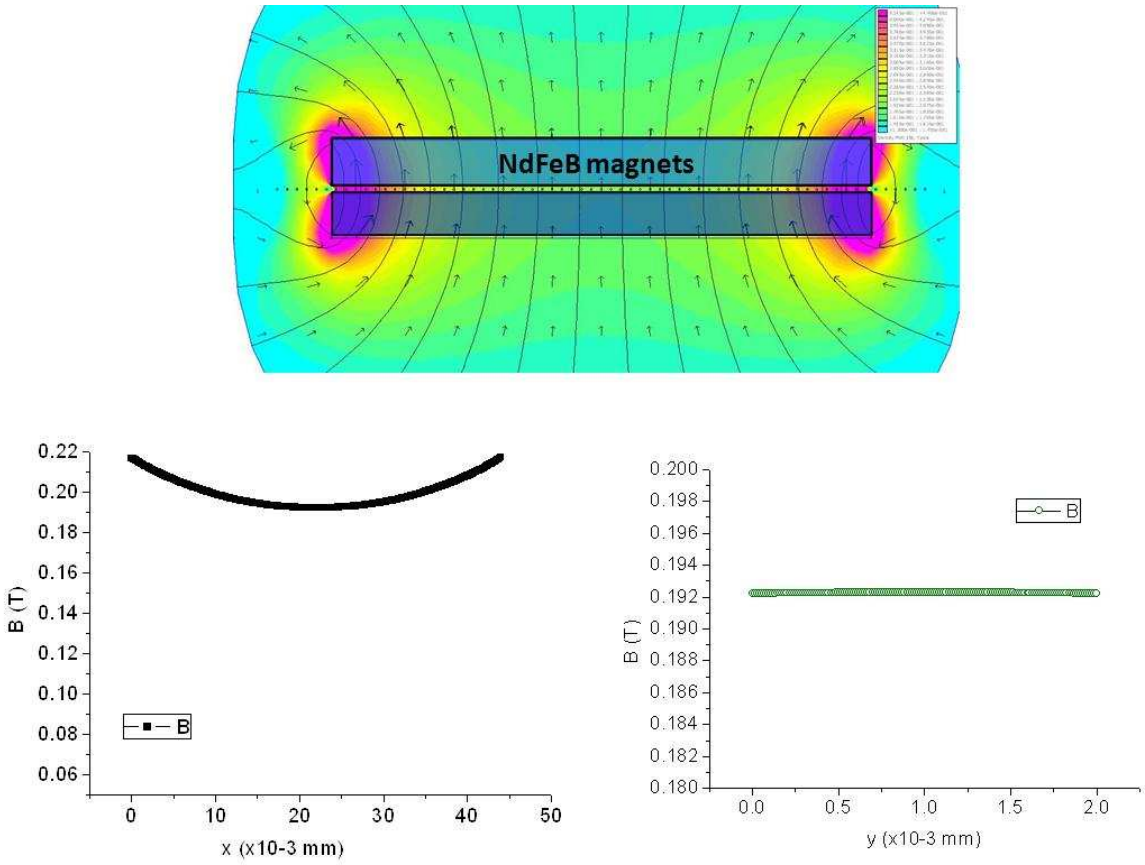

Figure 5. Representation of the magnetic field applied to the PC12 cultures. *The magnetic field was nearly constant in the y direction within values B= 0.19-0.20 T. The magnetic field gradient calculated from the numerical derivative of the B(y) curve was estimated to be* $\frac{dB}{dy} = 0.019 \frac{T}{m}$.

The central space was designed to fit the current sample holders, i.e., 6 cm T-25 flasks or 3 cm Ibidi Petri dishes (Figure 6).

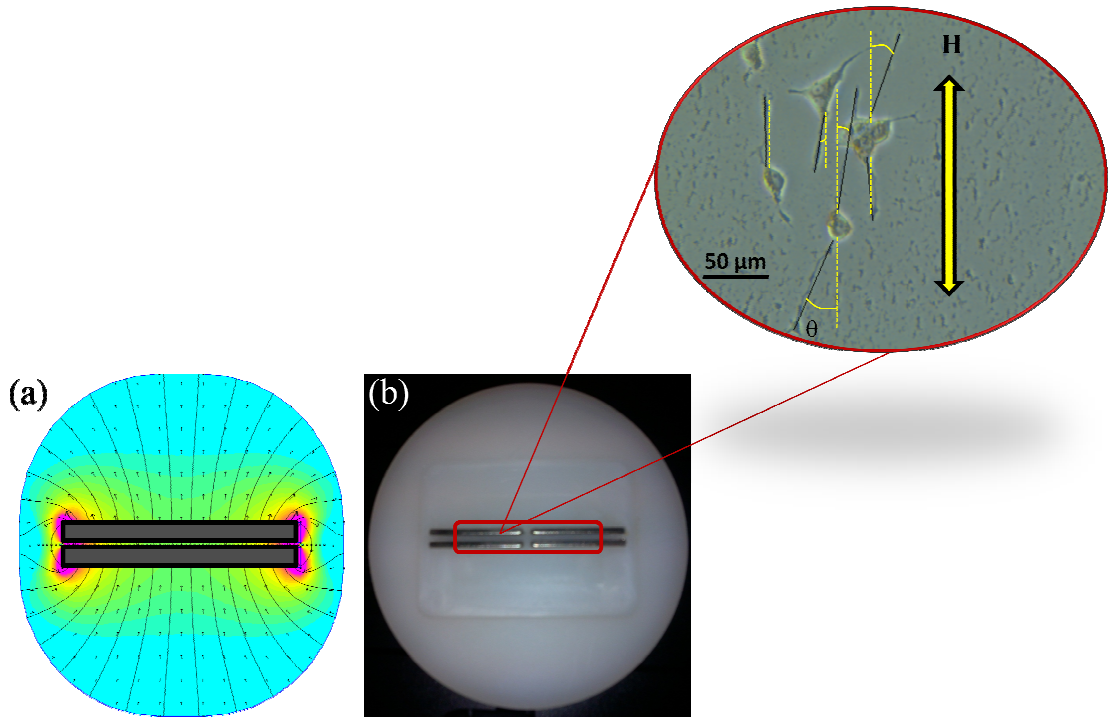

Figure 6. *(a) Representation of the magnetic field applied to the PC12 cultures. The magnetic field was homogeneous in Y and X direction (0.19-0.20 T). The maximum magnetic field gradient was 0.019 T/m. (b) Image of the support where the T-25 flasks were incorporated and an example of the images obtained by optic microscope in the area where the cells are analyzed. The image shows the analysis of the neurite length and neurite direction; each neurite is manually traced and then, the length and the angle formed between the neurite and the direction of the magnetic field (θ) are recorded.*

Four experimental conditions were tested: cells treated with both PEI-coated MNPs in presence of the magnetic field (MNP^+ H^+); cells treated with PEI-coated MNPs without magnetic field (MNP^+ H^-); cells without PEI-coated MNPs and in the presence of the magnetic field (MNP^- H^+); and cells without treatment (without MNPs and a null magnetic field, MNP^- H^-). Experiments were carried in a 4-plicate. For each experiment, around 60 pictures were acquired and around 250 neurites was counted. Neurite length and neurite number/cell were also measured. Analysis was performed by using image analysis software "Image J" (http://rsb.info.nih.gov/ij/). To asses neurite directionality and length, the neurites present in each sample analyzed were manually traced using the straight line segment tool of the program Image J (inset of Figure 6b), and their angles

of orientation were recorded and grouped into 20º angle bins from -90º to 90º. The direction of the angles was measured along and opposing the direction of the magnetic field. The analysis was done the 4th day after the induction of differentiation with NGF.

5. Statistical analysis

All values are presented as a mean ± S.D. All experiments were performed at least in triplicate**.**

IV. RESULTS

1. PEI coated Fe_3O_4 nanoparticles: synthesis process and physical characterization

In this work, PEI-MNPs were synthesized by a modification of the well known oxidative hydrolysis method [47] which consists of the oxidation of Fe $(OH)_2$ by nitrate in basic aqueous media. This method was modified by adding the branched polyethyleneimine polymer (PEI, 25 kDa) during synthesis reaction in order to synthesize PEI-functionalized Fe_3O_4 nanoparticles (PEI-MNPs) [14]. The presence of the polymer on nanoparticle surface determined the final surface charge, their resistance to aggregation, and the number of available functional groups on the particle surface. TEM images of the PEI-MNPs (Figure 7) showed that the particles were faceted displaying an octahedral shape. Statistical analysis of the particle size based on the size histogram revealed an average particle size of 25 ± 5 nm. From the HRTEM image of PEI-MNPs shown in Figure 7, it could be seen the presence of a thin layer (7 – 9 Å) of PEI coating around the Fe_3O_4 cores.

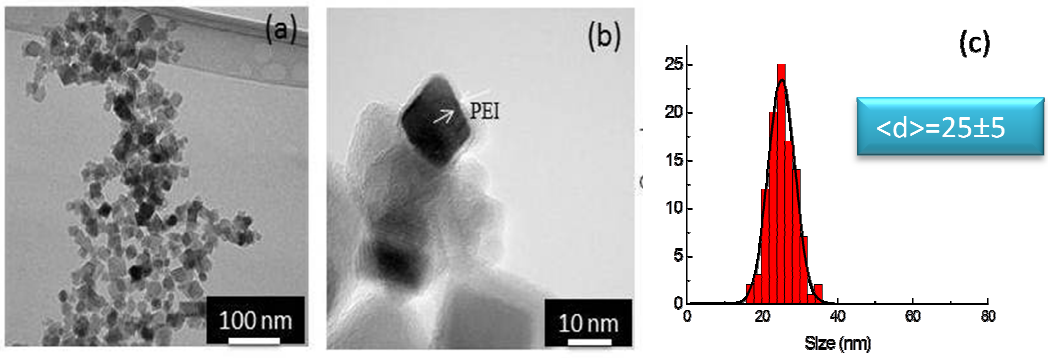

Figure 7. *(a) TEM images of PEI-MNPs, (b) HRTEM image. The arrows mark the layer of PEI coating the Fe_3O_4 MNPs and (c) histogram showing the size distribution of PEI-MNPs [14].*

From the Z-potential measurements it could be seen that the isoelectric point of PEI-MNPs is around 10.3. The high value of the isoelectric point and the positive charge value extended to lower pH values observed from the Z-potential data (Figure. 8) are in agreement with the presence of the PEI amino groups at the particle surface [14].

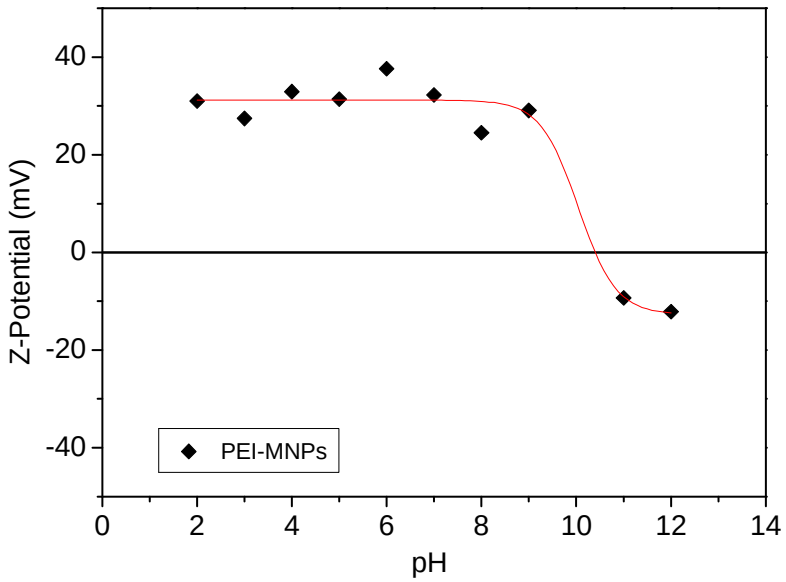

Figure 8. Z-potential values vs. pH for PEI-coated magnetic nanoparticles.
The lines are only a guide for the eye [14].

Previous work [14] on these MNPs showed that the hydrodynamic diameter obtained by DLS measurements, $\langle d_{DLS} \rangle = 70 \pm 15$ nm, indicating a low degree of agglomeration in the colloidal state consisting of 3-5 MNPs per cluster. This is in agreement with the high stability observed for the colloids, since larger agglomerates will led to fast precipitation.

The ZFC-FC curves of the particles (Figure 9) increased continuously with temperature with no evidence of a maximum up to 250 K, indicating that the blocking temperature is above room temperature. This is in agreement with the small but measurable coercive fields $H_C = 6.1$ kA/m observed from the hysteresis loops performed at T = 250 K (see the inset of Figure. 9 (a)).

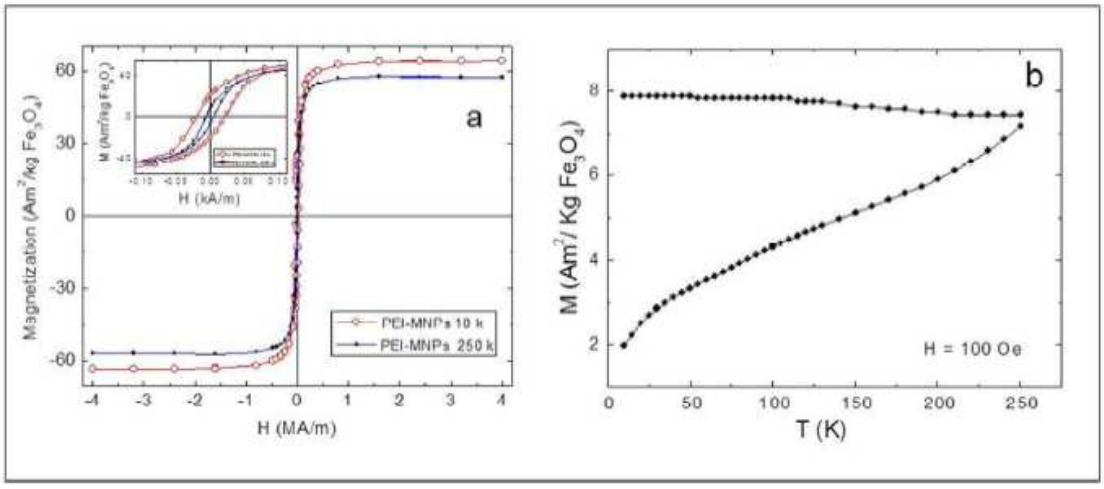

Figure 9. *(a) Magnetization curves at 10 and 250 K of PEI-MNPs. The inset shows the central area of the loop at higher magnification. (b) Zero-field and field-coated curves [14].*

Regarding the magnetic properties of the synthesized MNPs, it is worth to mention that the main parameters like saturation magnetization M_S and coercive fields H_C of the PEI-MNPs (sizes around 25 nm) was found to be smaller than the values of bulk magnetite (M_S = 86 – 92 Am^2/Kg, H_C = 16 – 32 kA/m) [6, 48]. These results are in agreement with the fact that possible contributions from surface disorder are expected to be almost negligible. Accordingly, the PEI-MNPs showed decreased values of M_S (58 Am^2/Kg Fe_3O_4 at 250 K), in agreement with the increased surface/volume ratio.

2. Neuronal (PC12) cells incubated with PEI-MNPs

2.1 Biological effects: cytotoxicity

Minimal cytotoxicity is another crucial requirement for any biomedical application. In a concentration range of 5-100 µg/mL, we found a negligible cytotoxicity (<5% for 100 µg/mL of particles added) after 72 h of incubation with the particles. At the concentration of 10 µg/mL (working concentration in further experiments) toxicity was less than the 1.5 % (Table 1) [39].

	10 μg/mL	*20 μg/mL*	*50 μg/mL*	*100 μg/mL*
Cytotoxicity (%)	1.4 ± 0.4	1.3 ± 0.5	2.2 ± 0.4	3.8 ± 0.8

Table 1. Effect of PEI-MNPs on PC12 cell line. *Cell viability was carried out by PI exclusion after 72 h of incubation. Cell counting was carried out using FACS analysis (mean ± s.e.m., n=6, p<0.0001).*

As a general result, the data on the viability of PC12 cells performed by Propidium Iodide exclusion assays (Table 1) displayed a toxicity level that increased in concentration-dependent manner. The toxicity was less at short incubation times but little important effects were noticed for incubation times longer than 48 h and large MNPs concentrations (Table 1). In spite of the effect for the largest MNPs concentrations, it is worth to note that these values correspond to incubation conditions (e.g., 72 hours and 100 μg/ml) that largely exceed therapeutic values.

2.2. Quantification of uploaded PEI-MNPs in neural cells

The intracellular iron content for the PEI coated MNPs in PC12 cell line is shown in Figure 10. After incubating cells with various concentrations of PEI-MNPs (from 5 μg/mL to 50 μg/mL of MNPs) in PC12 cells, we observed that when we increased the amount of PEI-MNPs incubated with the cells, the intracellular uptake of our positively charged MNPs also increased. Thus, significant nanoparticle internalization was observed for PEI-MNPs after 24 hours of nanoparticle incubation in the culture medium. It is possible that the PEI-MNP attachment to the membrane and the PEI-MNP internalization was facilitated by their positively charged surface. At the working concentration (10 μg/mL of PEI-MNPs), PC12 cells incorporated around 10 pg Fe per cell; this value includes both MNPs attached to the cell membrane by electrostatic attraction and MNPs inside the cell.

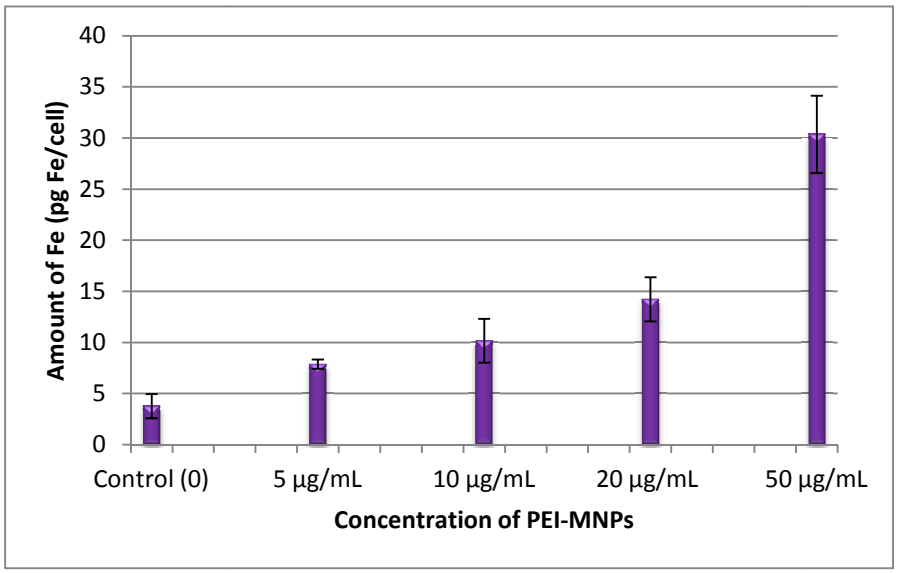

Figure 10. *Total amount of iron content per cell at different concentration of PEI-MNPs added.*

2.3. Biodistribution of PEI-coated MNPs in neuronal cells

The cellular localization of particles after incubating with PEI-MNPs at a concentration of 10 µg/mL was investigated using TEM analysis (Figure 11) [14].

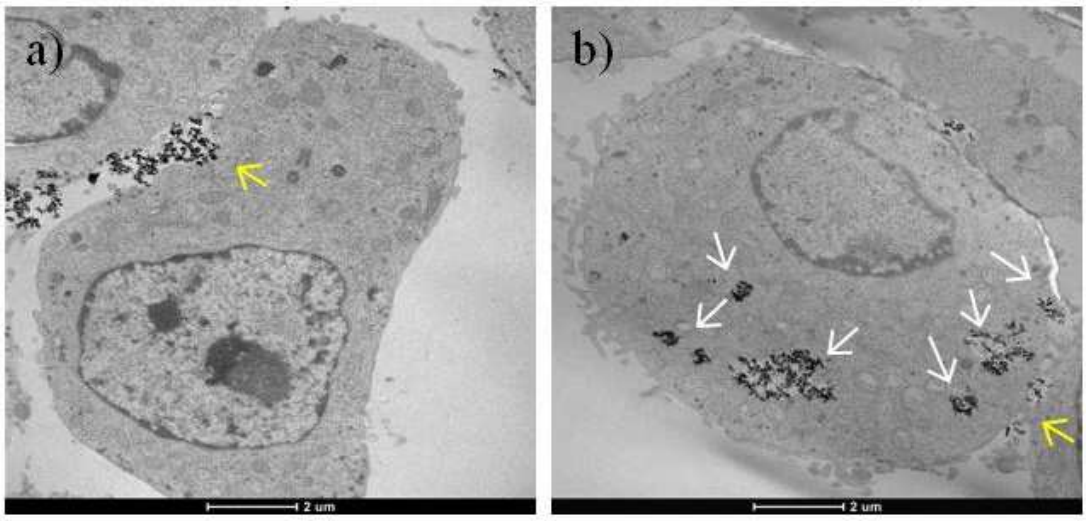

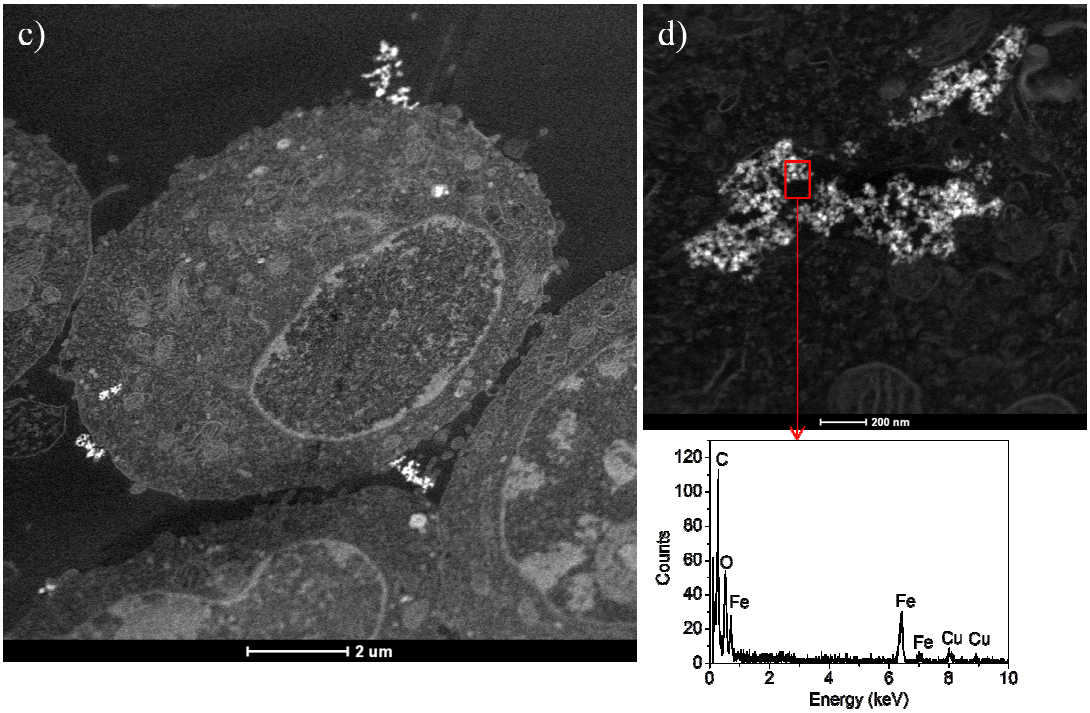

Figure 11. Cellular localization of PEI-MNPs*. a-b) TEM analysis of PC12 cells incubated 24 h with f-PEI-MNPs 10 µg/mL. White arrows: particles in the cytoplasm, yellow arrows: particles entering and membrane invagination; c-d) STEM-HAADF images (100 K) of PC12 cells incubated 24 h with PEI-MNPs 10 µg/mL. The inset of panel d) shows the EDS-HAADF spectra of citoplasmatic PEI-MNPs. The EDS-HAADF spectra confirm the presence of Fe inside the cell.*

TEM images revealed the presence of cluster of particles inside cells (Figure 11 a-b, white arrows) and on the cell membrane (Figure. 11 a-b, yellow arrows). No particles were detected in the nucleus. The presence of Fe inside the cells was confirmed by EDS–HAADF spectra (Figure 11 c-d).

The cellular localization of particles after incubating with PEI-MNPs at a concentration of 10 µg/mL was investigated using SEM and Dual Beam analysis. The PEI-MNPs biodistribution was investigated after incubation in two conditions: cell cultures with PEI-MNPs for 24 h, differentiated by NGF induction and without external magnetic field (named MNP^{+} H^{-}); the other condition was cell cultured with MNPs for 24 h, differentiated by NGF induction and differentiated in the presence of an external magnetic field (named MNP^{+} H^{+}).

SEM images showed that after incubation, a fraction of PEI-MNPs were strongly attached to the soma and growth cone in both, control cells (without magnetic field) and cells subjected to magnetic field, forming large clusters ranging from 1 to 5 µm in

length. In agreement with SEM images, EDX analysis confirmed that these bright spots were PEI-MNPs and were strongly attached to the cell membrane (Figure 12). Red color gives us an idea of the amount of iron over the cell.

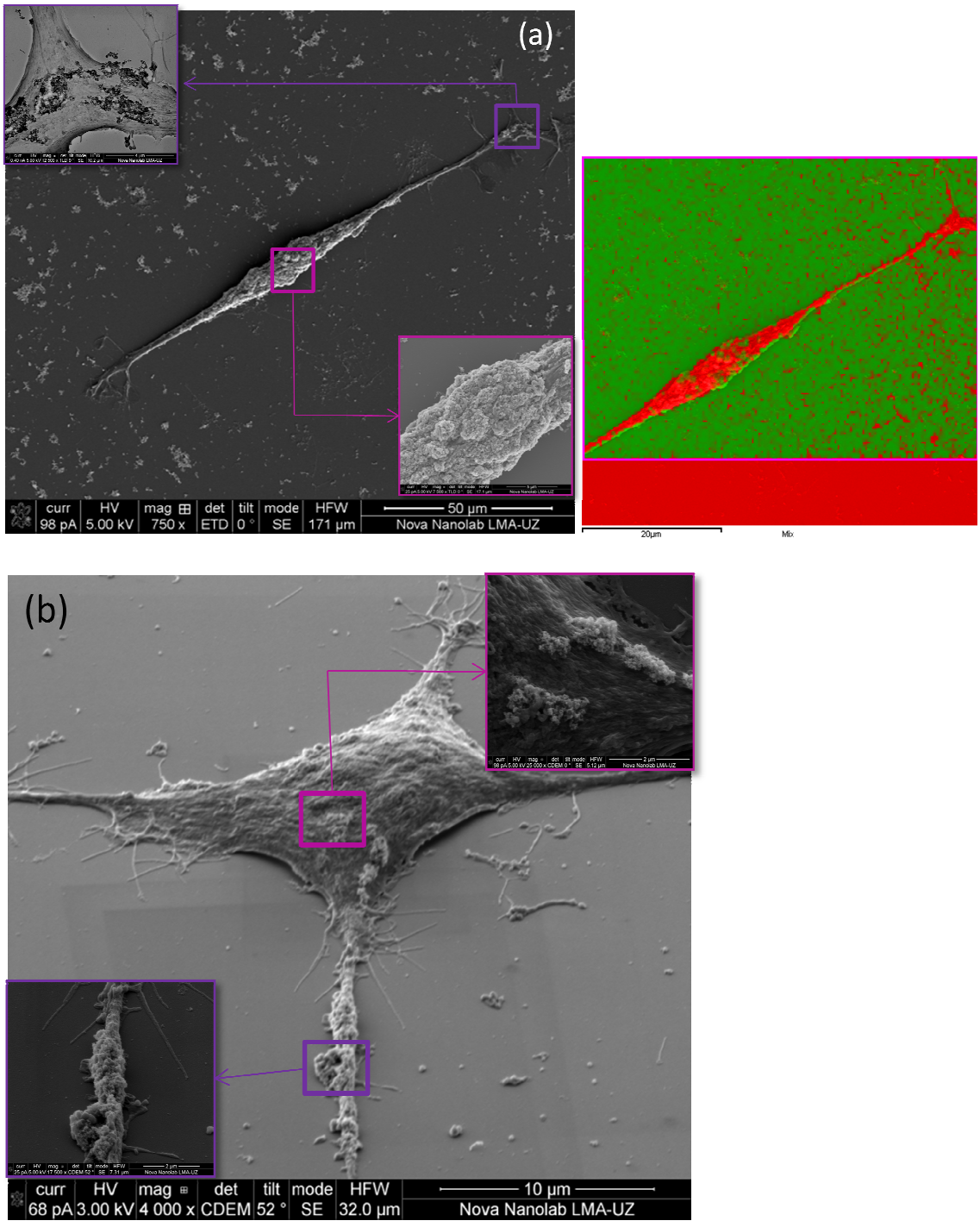

Figure 12. Scanning electron microscopy image of a single PC12 cell incubated for 24 hours with 10 µg/mL PEI-MNPs, showing the presence of PEI-MNPs agglomerates (bright spots) on the cell membrane and on the growth cone. *(a) PC12 cells without magnetic field and EDX analysis showing Fe in red and O in green. (b) PC12 cells subjected to magnetic field.*

The combination of Ion and Electron beam (SEM/FIB) allows the study of the internal distribution of particles in adherent cells because it allows us to see the PEI-MNPs inside the cross-sectioned cells.

For further study of the internalization of the PEI-MNPs, single PC12 cells were cross-sectioned by FIB and analyzed by SEM after culture in the presence of 10 µg/mL of PEI-MNPs for 24 hours. The results were different for PC12 cells cultured in the presence of an external magnetic field (MNP^+ H^+) and PC12 cells cultured without magnetic field (MNP^+ H^-). In the Figure 13 it is possible to observe the agglomeration of the PEI-MNPs attached to the outside part of the cell membrane in MNP^+ H^- condition, and also the agglomerates could be seen along the intracellular space of the neural soma. It is important to point out that we did not find MNPs in the intracellular space of the axon, we only found MNPs in the intracellular part of the neural soma of MNP^+ H^- cells.

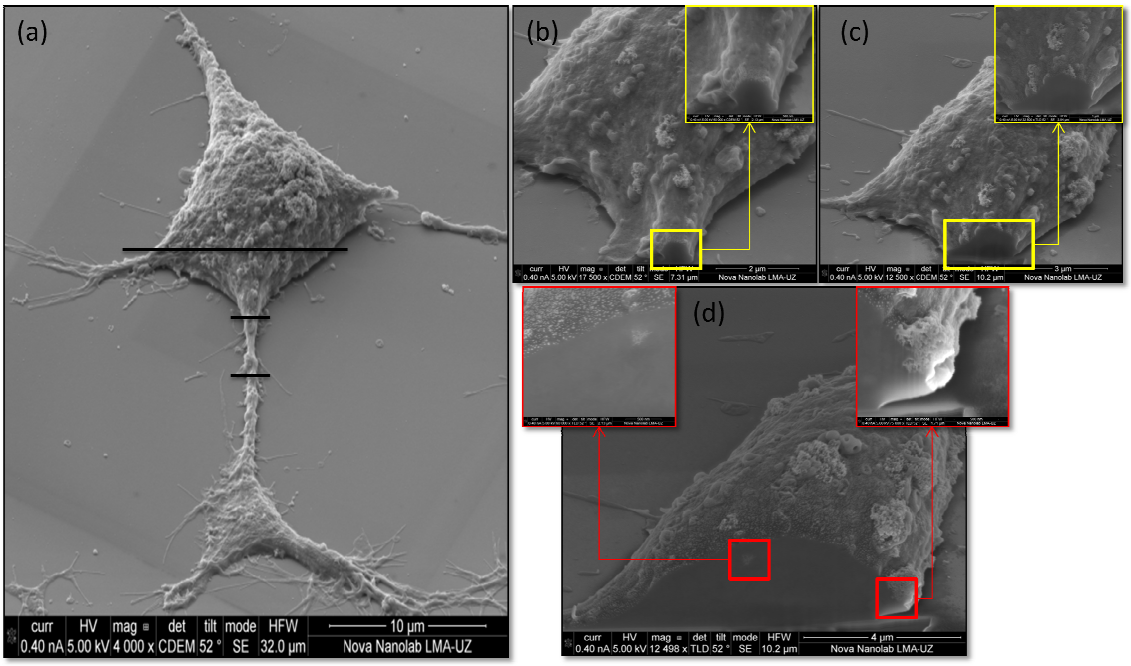

Figure 13. SEM images of PC12 cells (MNP^+H^-) cross-sectioned by FIB after 24 hours incubation at 10 µg/mL of PEI-MNPs and for 4 days of differentiation. *(a) The whole cell at 52 º tilted previously to be cross-sectioned. (b) And (c) intracellular space of the axon in where we could observe the absence of PEI-MNPs. (d) Neural soma intracellular space in where we could see the presence of PEI-MNPs in both attached to the membrane and in the intracellular space.*

As we can see in the Figure 14 (see also Figure A1), in the case of MNP^{+} H^{+} condition, we could find agglomeration of the MNPs in the intracellular part along the whole cell to occupy a major fraction of the intracellular space. EDX spectra showed that these agglomerates were composed of iron. The MNPs distribution observed consisted of MNPs agglomerates attached to the cell membrane, which seem also to penetrate to the intracellular space of the soma and the axon.

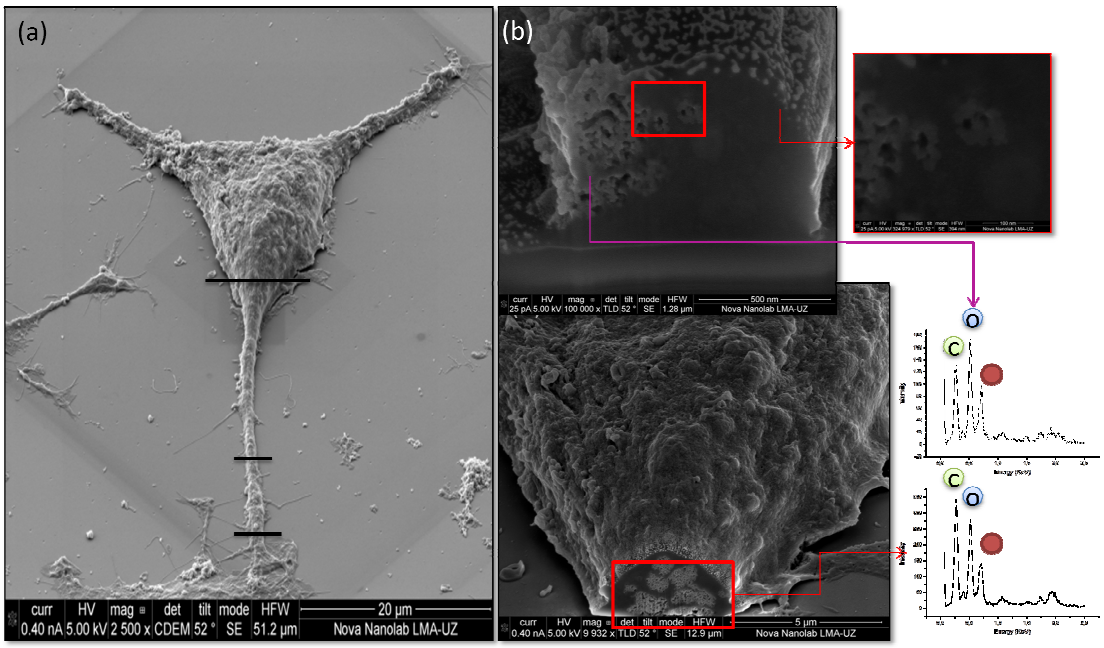

Figure 14. SEM images of PC12 cells ($MNP^{+}H^{+}$) cross-sectioned by FIB after 24 hours incubation at 10 µg/mL of PEI-MNPs and for 4 days of differentiation. *(a) The whole cell at 52 º tilted previously to be cross-sectioned. (b) Intracellular space of the axon in where we could observe the presence of PEI-MNPs agglomerates in both attach to the membrane and inside the axon. (c) Neural soma intracellular space in where we could see the presence of PEI-MNPs. The insets correspond with the EDX spectra of the highlight part.*

The microscopy imaging analysis of the PEI-MNP-loaded PC12 cells indicated that the kinetics of particle uptake could go through progressive stages like a) a first attachment to the cell membrane as clearly observed from SEM images; b) a subsequent membrane crossing reflecting early endocytosis (with pathways not yet known), and c) progressive accumulation in membrane-bound intracellular vesicles. The detailed mechanisms through which MNP uptake is mediated by PEI is still to be determined.

The results from SEM and Dual Beam microscopy (Figure 13 and 14) showed that, after incubation the final distribution at the cellular level consisted of large agglomerates of

PEI-MNPs both attached to the cell membrane and at the intracellular space. The capacity provided by the Dual Beam technique, of analyzing the biodistribution of the MNPs at the single-cell level, demonstrated also that the agglomerates observed outside the cellular membrane extended in a continuous way into the cytoplasm. The results also showed that the magnetic field promote the retention and accumulation of PEI-MNPs in cells and can facilitate the movement of these PEI-MNPs from the soma to the axon growth cone or their incorporation in the axon. The combination of PEI-MNPs and an external magnetic field can provide mechanical tensile forces in the growth cone that may cause axonal sprouting [49].

Since the PEI-MNPs did not show major toxicity effects except for the largest concentrations and after long incubation time (72 h) [14], the final distribution of large magnetic agglomerates anchored to the PC12 cells opens the possibility of using external fields for cellular actuation through external magnetic forces on these structures.

These results also confirmed that there were no particles in the nucleus.

2.4. Immunofluorescence analysis of neuronal cell cytoskeleton

Morphological changes in the PC12 cells during differentiation were also affected by the PEI-MNPs (Figure 15 and Annex section, Figure A2). These differences could be observed and analyzed through phase contrast and immunofluorescence microscopy. Typical PC12 cells, prior to NGF exposure, are undifferentiated, spherical in shape and do not produce neurites, as can be seen in Figure 15a. Following exposure to NGF, as shown in Figure 15b, PC12 cells differentiate into neuronal type cells (+NGF) and begin to extend short and thin neurites (5-6 per cell) into the periphery. PC12 cells exposed to PEI-MNPs were more elongated, showed less number of neurites (around 2-3 per cell), and these were longer and sharper (Figure 15c).

The number of connections or neuronal synapses also increased in the presence of MNPs.

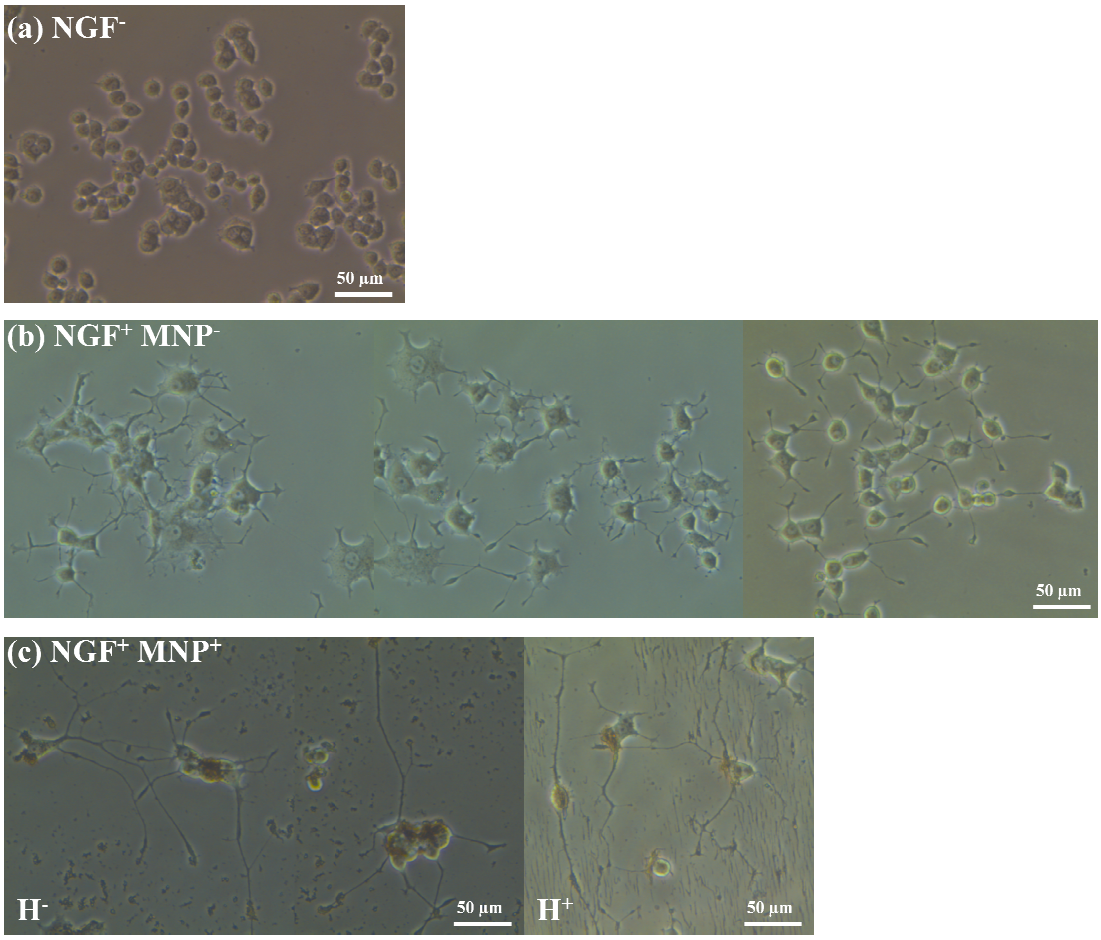

Figure 15. Phase contrast images of PC12 cells: *(a) undifferentiated, (b) with NGF (NGF^+, $MNPs^-$), (c) with NGF and PEI-MNPs (NGF^+, $PEI\text{-}MNPs^+$). The b and c images were recorded the 4^{th} day of inducing differentiation. These results indicate that PEI-MNPs promoted neurite outgrowth relative to non-treated cells.*

PC12 cells incubated with PEI-MNPs and differentiated in the presence of the magnetic field exhibited neurites outgrowth in the direction of the applied magnetic field (Figure 16 and Annex section, Figure A3). Neurites of PC12 cells did not treat with PEI-MNPs but differentiated in the presence of the magnetic field displayed higher number of neurites and randomly oriented (Figures 15 and 16).

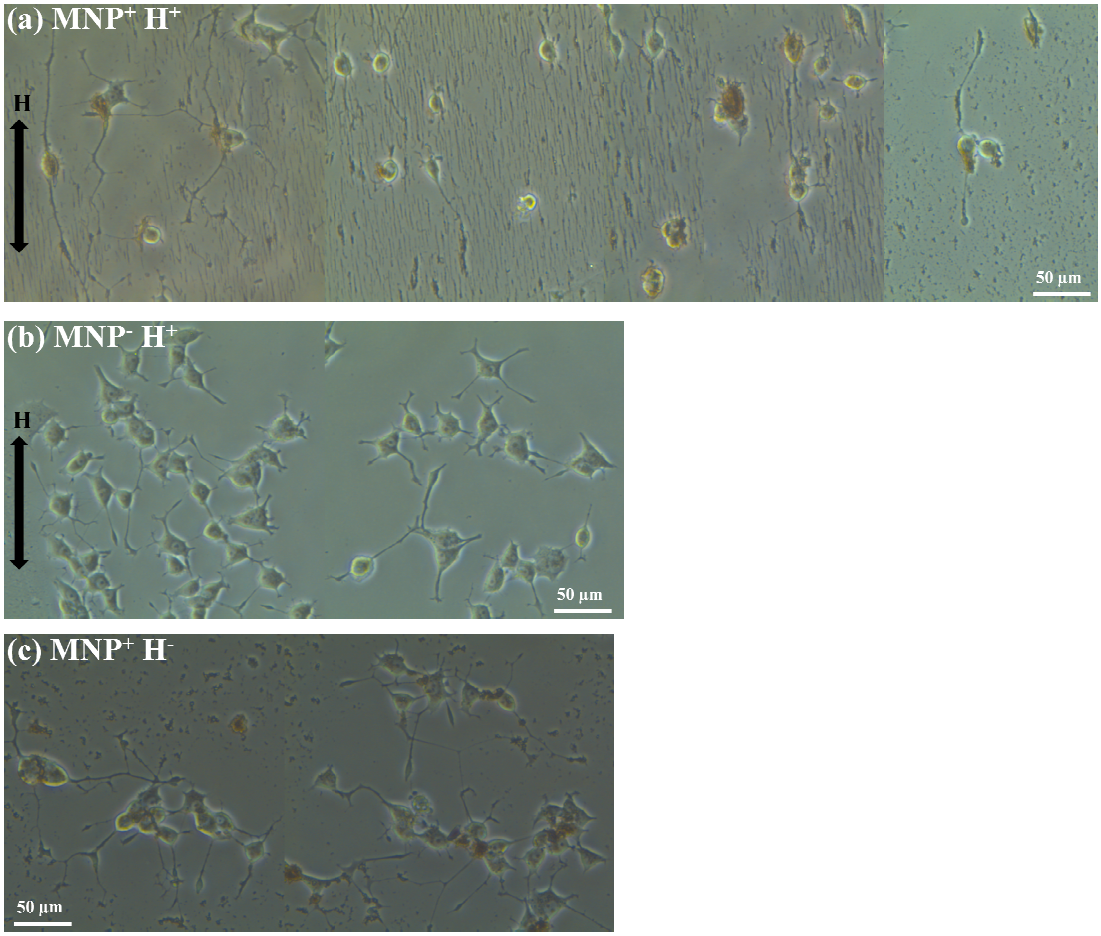

Figure 16. Phase contrast images of PC12 cells: *(a) incubated with PEI-MNPs and differentiated in the presence of a magnetic field (MNP^+ H^+), (b) differentiated in the presence of a magnetic field (MNP^- H^+) and, (c) incubated with PEI-MNPs in the absence of an external magnetic field (MNP^+ H^-).*

The changes in morphology and cytoskeletal structure of cells exposed to PEI-MNPs and a magnetic field (H) were also investigated using immunofluorescence for β tubulin and F-actin. The cells were fixed, permeabilized and stained with fluorescently labeled secondary antibody to primary anti-tubulin antibody-labeled microtubules, while actin microfilaments were labeled with phalloidin (Figure 17 and Figures A4 and A5, Annex section).

Untreated cells (MNP^-) exhibited strong peripheral F-actin staining along the cell edge, indicative of cortical actin fibers. Also, the actin microfilaments were well organized on the top of neurites forming filopodia and lamellipodia (Figure 17).

At the same day of differentiation (4th day) untreated cells exhibited spherical unpolarized shape and, had short undifferentiated neurites (Figure 17a). The microtubules also form a dense network equally distributed around the nucleus and along the neurites of the cells (Figure 18). In the case of cells incubated with PEI-MNPs (MNP^{+}), there were prominent filopodia and lamellipodia on the top of neurites; the cells were polarized and possessed two types of morphologically and functionally distinct processes; a single, long, and slender axon and several dendrites that are shorter processes with a tapered morphology (Figure 17b).

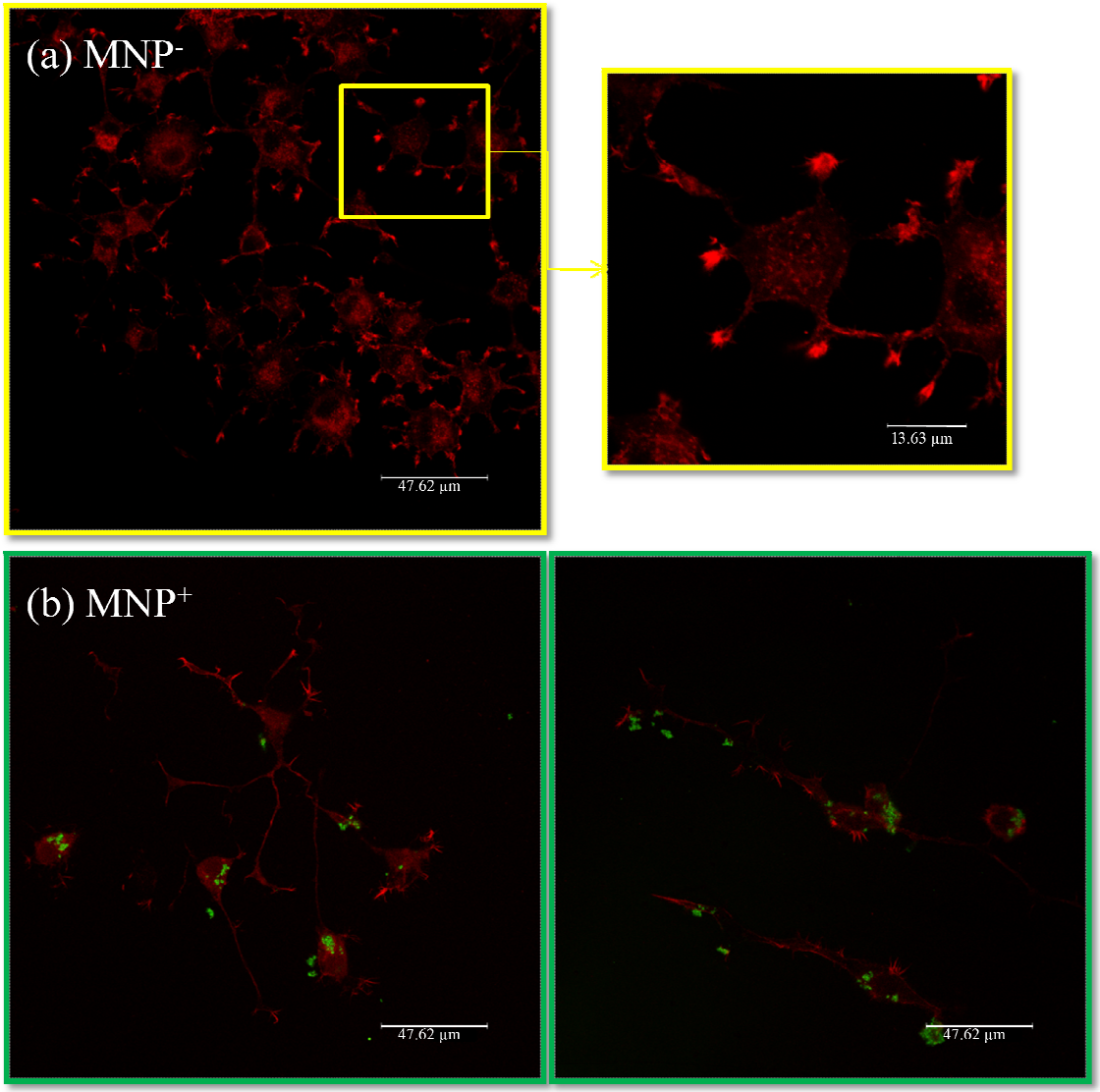

Figure 17. Immunofluorescence images of differentiated PC12 cells 4 days *control (a) and after treatment with f-PEI-MNPs (b). Red fluorescence represents actin microfilaments and green color represents fluorescent nanoparticles. (a) PC12 cells without f-PEI-MNPs treatment; the inset of (a) is a detail of PC12 cell that exhibited spherical unpolarized shaped*

with short neurites. (b) PC12 cells treated with f-PEI-MNPs; cells exhibited typically neuron shape with a long slender axon and several shorter dendrites.

Confocal images also confirmed the internalization of the f-PEI-MNPs inside the cell. It is important to point out that f-PEI-MNPs were found along the length of the body cell, in both, the intracellular part of the neural soma and the neurites, but specially in the neural soma and never in the inner of the nucleus.

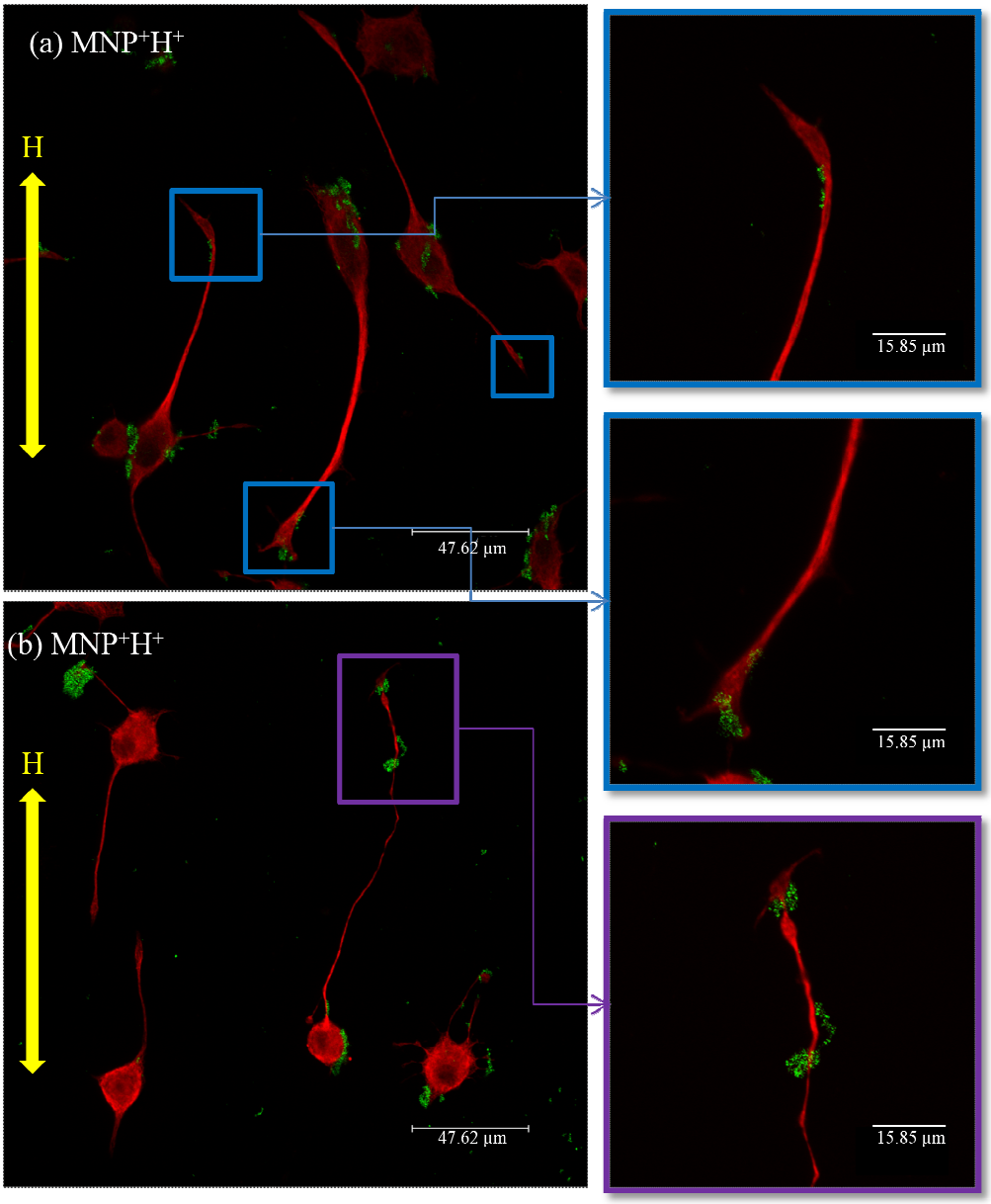

Figure 18. Immunofluorescence images of differentiated PC12 cells 4 days after treatment with f-PEI-MNPs in the presence of magnetic field (MNP^+ H^+). *Red fluorescence represents tubulin microtubules and green color represents fluorescent nanoparticles and yellow line*

represents the magnetic field direction. (a) And (b) MNP^+ H^+ PC12 cells stained with anti-tubulin III antibodies. The images on the right represent the detail of axon of the PC12 cells in which it is observed the PEI-MNPs inside the axon.

3. Control of the orientation of growing neuronal processes in PC12 cell line

To demonstrate that the synergic combination of PEI-MNPs and magnetic field can influence the orientation of the neuronal processes of PC12 cells incubated with PEI-MNPs, the neural cells were exposed to a constant magnetic field of 0.19-0.20 T and to a maximum magnetic field gradient of 0.019 T/m (the configuration of the magnets is shown in the section 4 of Materials and Methods).

For these experiments, PC12 cells were treated with PEI-MNPs (10 μg/mL) for 24 hours; then PC12 cells were induced to differentiate by adding NGF (80 ng/mL) and an external static magnetic field was applied for 5 days. Four experimental groups were tested: cells treated with both PEI-MNP and the magnetic field (MNP^+H^+), with MNP and a null magnetic field (MNP^+H^-), without MNPs and the magnetic field (MNP^-H^+) or without MNPs and a null magnetic field (MNP^-H^-). The results obtained from cells treated with MNPs and magnetic field (MNP^+H^+) were compared with cells treated with magnetic field but without MNPs (MNP^-H^+), cells treated with MNPs but without magnetic field (MNP^+H^-) and control cells without treatment (MNP^-H^-). Finally, the angle between the direction of each neurite along the magnetic direction and the neurite length were measured the 4th day after the induction of differentiation by optic microscope and the analysis was performed by using image analysis software “Image J” (Figures 19, 20, 21 and 22).

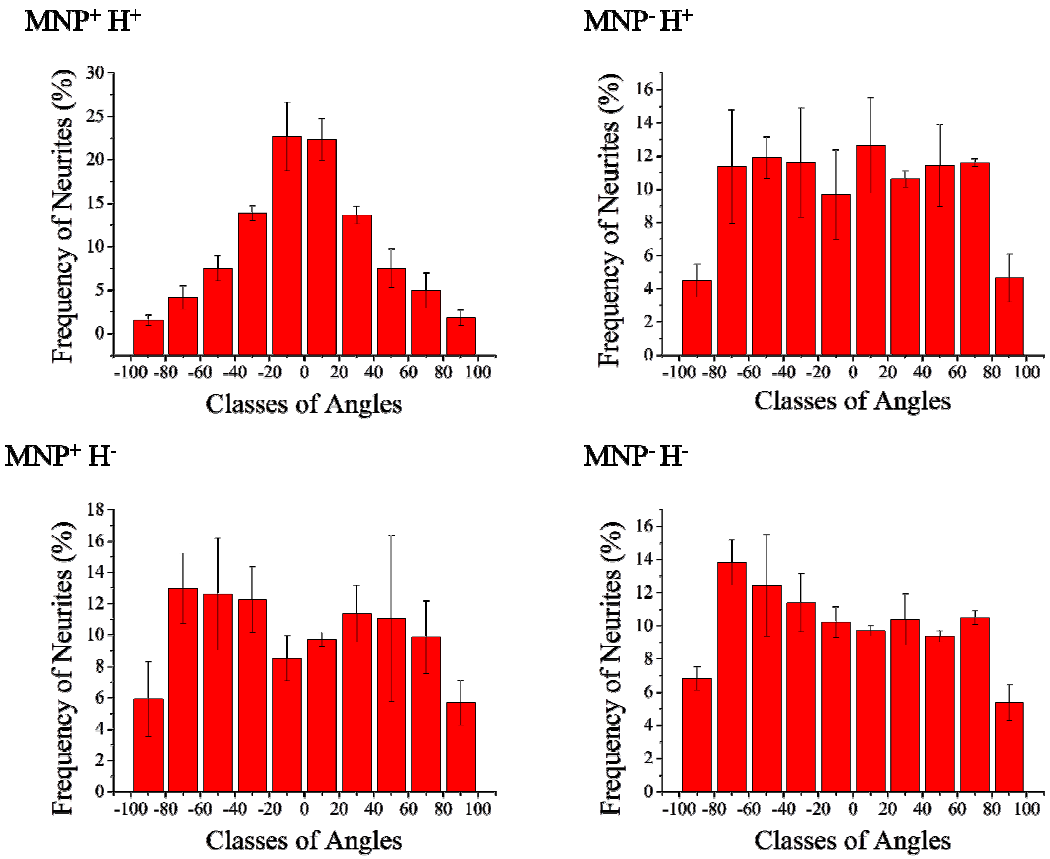

Figure 19. Representation of the results obtained in each condition by using "Image J". *The graphs show the percentage of neurites as function of the angles along the direction of the static magnetic field applied. Data are grouped for classes of angles from -90º to +90º. The direction of the magnetic field is 0º (mean ± SD., n=3-6,).*

As we can see in Figure 19, when an external magnetic field was applied to PC12 cells that previously had been treated with PEI-MNPs, and had loaded them their neurites were able to orientate in the direction imposed by the external magnetic field, so the neuronal processes of PC12 cells tended to be arranged parallel to one another and parallel to the magnetic field. In the other conditions, without PEI-MNPs or without magnetic field, the neurites were randomly oriented and approximately the same number of neurites was found in each class of angle. The $MNP^{+}H^{+}$ condition graph followed a normal distribution (Figure. 20), so under the magnetic field, we could calculate the preferential orientation angle of the neurites which was 0.0846 ± 34.20 º.

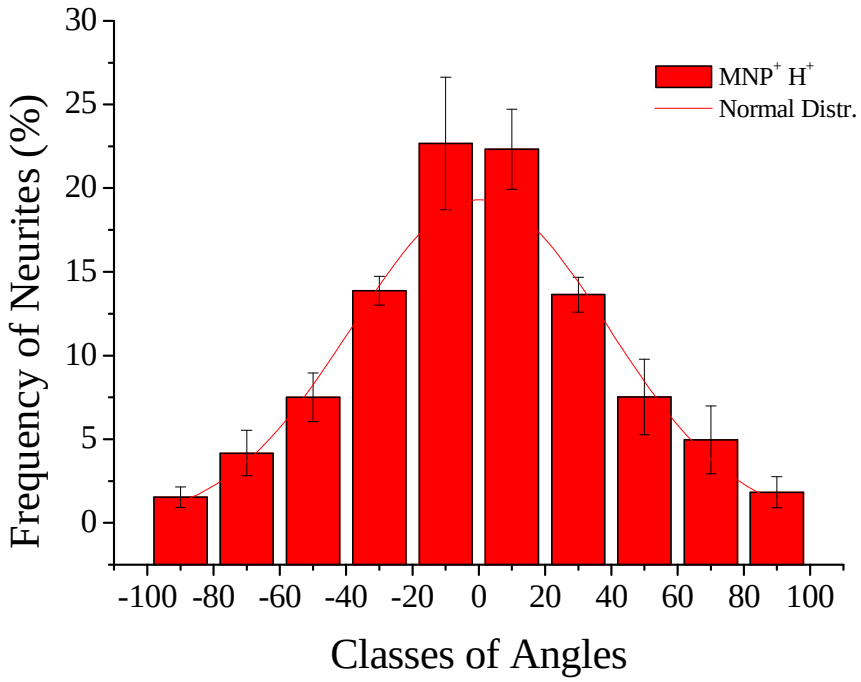

Figure 20. Representation of the results obtained in the cells treated with PEI-MNPs and magnetic field (MNP$^+$H$^+$) by using "Image J". *The graph shows the percentage of neurites as function of the angles they form with the direction of the external magnetic field and the fitting of the data to a normal distribution in order to obtain the neurite preferential angle of orientation. Data are grouped for classes of angles. The direction of the magnetic field is 0º.*

The same results are represented in Figure 21 in term of number of neurites (normalized with respect to the control: MNP$^-$ H$^-$) in each condition as function of the angles.

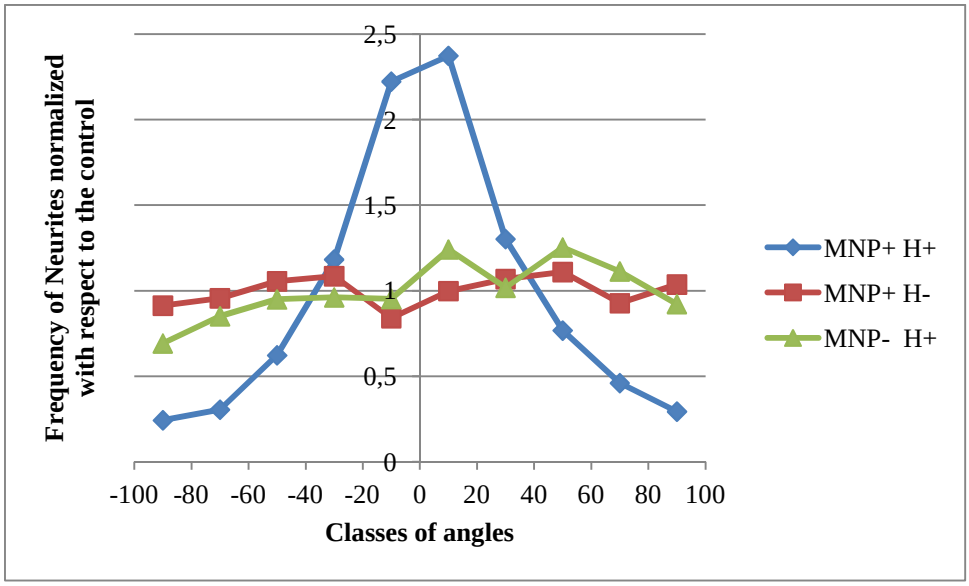

Figure 21. Number of neurites (normalized with respect to the control) as function of the angles. *Data are grouped for classes of angles.*

All representations allow the conclusion that in the presence of both PEI-MNPs and magnetic field, neurites preferentially grew during the neural processes in the direction imposed by the external magnetic field. As expected, three controls were not significantly different indicating that magnetic nanoparticles or magnetic field alone did not influence the direction growth of the neurites.

Neurite length was also affected by the PEI-MNPs. Figure 22 show the percentage (%) of neurites as a function of length of neurites in the four experimental conditions tested. The analysis of neurite population revealed that the percentage of cells with neurites lengths between approx. 80 and 140 μm increased for those cells incubated with PEI-MNPs (Figure 22). The neurites of the cells incubated with PEI-MNPs, in MNP^+ H^+ and MNP^+ H^- conditions, were larger than the neurites of the PC12 cells did not treat with nanoparticles (MNP^- H^+ and MNP^- H^- conditions) (Figure. 22). The median lengths (calculated adjusting the data to a log normal distribution) of neurites of cells incubated with PEI-MNPs were 7 μm longer than the neurites of cells untreated with PEI-MNPs; moreover, if the cells were differentiated in the presence of an external magnetic field, the length of neurites increased, and were 10 μm longer than the neurites of the control cells. However, there were not significant differences between the neurite length of cells not treated with PEI-MNPs but differentiated with or without the presence of the magnetic field. This means that the application of magnetic field not only had influence on the neurite orientation but also it had on the amount of neurite outgrowth (mean number of neurites per cell and the same length as the control) in PEI-MNPs-loaded cells (Figure 22).

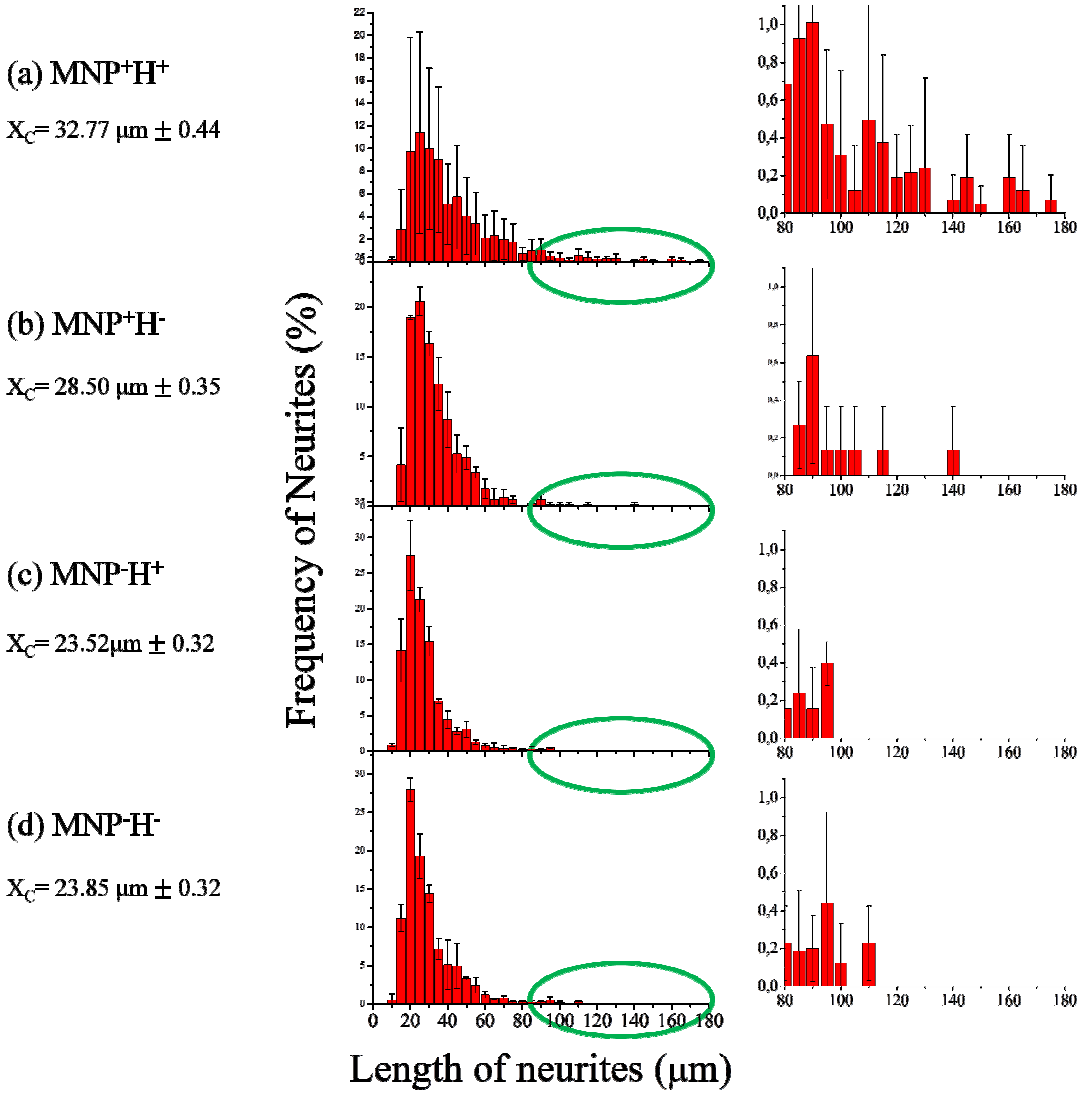

Figure 22. Analysis of neurite length distribution 4 days after the induction of differentiation *with NGF: (a) (MNP^+H^+); (b) (MNP^+H^-); (c) (MNP^-H^+); (d) (MNP^-H^-). (mean ± SD., n=3-6). Frequency of neurites vs. length of neurites is log normally distributed (the inset shows an amplification view of lengths 80-180 µm).*

V. DISCUSSION

The work reported here has been conceived within the wider framework of a research project aimed to validate a novel protocol for nerve regeneration based on the use of magnetic nanoparticles and external static magnetic fields. The hypothesis on which this research project was based is schematically depicted in Figure 23. When an injury occurs to a peripheral nerve, magnetic nanoparticles can be used to guide the regenerating axons across the traumatic gap by exposure to a magnetic field which exerts a magnetic force in the direction of the regenerating axon (from the proximal end to the distal portion). MNPs create a mechanical tension which stimulates nerve regeneration in the direction imposed by the magnetic field. This physical guidance should direct more efficiently the regeneration of the injured nerve from the proximal toward the distal stump. Additionally, MNP binding to the neuronal cells can be enhanced with addition of biological molecules, e.g., neural binders and neurotrophic factors (NF).

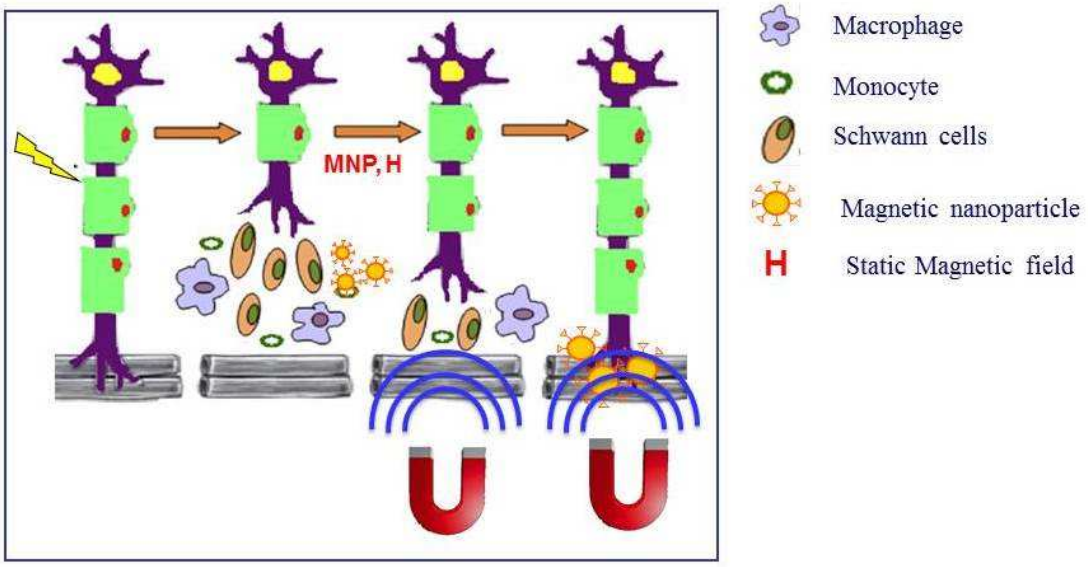

Figure 23. Nerve regeneration mediated by MNPs. *After a nerve transaction, Schwann cells, macrophages and monocytes work together to remove myelin debris, release neurotrophins, and lead axons toward their synaptic targets. MNPs bind the injured nerve, a magnetic field is thus applied in the direction of the nerve regeneration. MNPs create a mechanical tension which stimulates nerve regeneration in a direction imposed by the magnetic field. This physical guidance should direct more efficiently the regeneration of the injured nerve from the proximal toward the distal stump.*

Additionally, MNP binding to the neuronal cells can be enhanced with biological molecules, e.g., neural binders and neurotrophic factors (NF).

Although many types of magnetic nanoparticles are currently used in clinical protocols, the use of iron oxides nanoparticles in neurosciences is still limited due to the need of clear data on possible toxicity effects, the effects of poor water solubility and the nanometric size. Therefore the potential adverse effects of iron oxide nanoparticles are currently the focus of intense investigation [50], and measures to reduce adverse effects still remain explored [51].

Within this context, the present work was aimed to constitute a proof of principle for the magnetically-driven neurite orientation. Specifically, neuronal PC12 cells loaded with PEI-coated magnetic nanoparticles (PEI-MNPs) were used in order to demonstrate that a static magnetic field can orientate the orientation of neurites outgrowth in an *in vitro* model.

A first issue to note from the systematic analysis of different microscopic techniques (TEM, SEM, Dual-beam, confocal, fluorescence) is that there is a strong interaction between PEI-MNPs and PC12 cells. The results obtained from SEM and Dual Beam microscopy (See Figures 12, 13 and 14 of Results section-) showed that after incubation with MNPs the final distribution at the cellular level consisted of large agglomerates of MNPs both attached to the cell membrane and at the intracellular space. Indeed, the agglomeration of MNPs in biological media is an unavoidable process since the large concentration of proteins in cell culture media inevitably led to the formation of a protein 'corona' and, more generally, the formation of large aggregates. It is this kind of aggregates that constitute the entities to interact with cells and tissues in biological applications.

The analysis of the biodistribution of MNPs at the single-cell level through Dual Beam technique demonstrated that the agglomerates observed outside the cellular membrane extended in a continuous way into the cytoplasm. Since the MNPs resulted in a very low toxicity effects at the concentrations used for these experiments, the final distribution of large magnetic agglomerates anchored to the PC12 cells seems to be potentially useful for cellular actuation through external magnetic forces. The

internalization of these particles was also demonstrated by confocal microscopy. Interestingly, after incubation of the cells with PEI-MNPs and differentiation in the presence of an external magnetic field, we observed an enhanced presence of MNPs localized at the intracellular part of neural soma and axon.

The experimental results confirmed that the synergic application of MNPs and magnetic field gradient influence the orientation of the neurite growth. When cells were treated with the PEI-MNPs and exposed to the external magnetic field, the neurites tended to grow parallel to the field direction (see Figures 19, 20 and 21 of Results section 3). The experimental controls demonstrated that the magnetic field alone did not influence the direction of the neurites growth.

An influence of static magnetic fields onto the direction of newly formed neuronal processes of PC12 cells was reported by Kim et al. [46]. Specifically, the authors found that neurite grew preferentially in a direction perpendicular to the direction of the magnetic field. Unfortunately, the results cannot be compared because the experimental set-ups are different. Here the configuration of the magnets were designed in order to have a maximum magnetic field gradient (0.019 T/m) in the culture dish, i.e., all cells were exposed to the same magnetic force which is proportional to the magnetic field gradient and independent from the magnetic field value. On the opposite, Kim and colleagues used 12-well plate place between two permanent magnets with opposing poles facing each other to generate a magnetic field gradient (0,12 T at the center) and thus a magnetic force not constant.

The morphological changes in the PC 12 cells observed during differentiation and when PEI-MNPs were added to the cell culture were already mentioned in Section 3.2 of Results. It is clear from the analysis of the neurite length distributions that a measurable increase in the average neurite length was induced on the PEI-MNPs-loaded cells when compared to the different control samples (i.e., blank cells with no MNPs, with and without applied external magnetic field). The differences of average neurite lengths between control and MNP-loaded samples (see Figure 22 of the Results section 3) was found to be about 10 μm (control length: 23-24 μm; MNP-loaded samples length: 32-33 μm). These differences were observed irrespective of the presence of magnetic field, indicating that its origin is related to the incorporation of MNPs. This observation (that

the presence of the PEI-MNPs during cell differentiation improves the outgrowth of the neurites) suggests that the PEI-MNPs could have positive effects on neurite growth, but determining the exact source of this enhancing neurite factor would need further investigation. This is consistent with a previous work by Kim et al. [37] reported that MNPs alone (i.e., in the absence of the magnetic field) was able to enhance the neurite outgrowth in a dose-dependent manner on PC12 cells exposed to both MNPs and NGF. They concluded that treatment of PC12 cells with iron ion promotes neurite outgrowth during NGF-induced differentiation by enhancing cell attachment and survival via activation of cell adhesion molecules. Indeed, it has been reported [52, 53] that Fe ions can affect the neural plasticity and neurite outgrowth, but the molecular mechanisms of this influence has not been described in detail. Some groups have reported that the treatment of PC 12 cells with iron ion promoted neurite outgrowth during NGF-induced differentiation by enhancing cell attachment and survival [52, 53]. Since, it is possible that iron oxide nanoparticles can be ionized due to the acidic pH inside the endosome or lysosome and the Fe ions can be released into the cell cytosol. These studies concluded that iron oxide nanoparticles might enhance neurite outgrowth by increasing the intracellular concentration of Fe ions during the differentiation process [52, 53]. However, it is still possible that the iron oxide nanoparticles activate the extracellular receptor that in turn may induce the subsequent signal transduction for neurite outgrowth [37]. Further studies are necessary to identify the key factors that affect the differentiation pathway by iron oxide nanoparticles.

In spite of the increased value of the average neurite length observed for MNP-loaded PC12 cells, the average number of neurites $<N_N>$ counted for the same PC12 cells incubated with PEI-MNPs was smaller than the corresponding average neurite number in control cells.. The diminution of neurite formation after treatment with MNPs was also observed by Pisanic and co-workers [54]. They reported that the presence of intracellular anionic-MNPs appears to affect cytoskeletal structure by either chemically or physically impeding actin microfilament formation in the cells or inhibiting the maturation and function of neurites.

It is clear from the experimental results that the driving force guiding the neurite growth along the magnetic field direction is the force exerted on the incorporated magnetic nanoparticles by the external magnetic field. In other words, the preferred orientation is

based on the interaction between the magnetic moment of the MNPs and the external magnetic field. However, the detailed biochemical mechanisms by which these forces acting on the MNPs translate into a preferential growth direction for a large fraction of the neurites is not yet fully understood.

Some models have been proposed to simulate how a mechanical stimulation can activate cellular signaling pathways that are known as mechanotransduction pathways [41]. The process by which cells convert physical force into a biochemical signal plays a key role in the outgrowth and migration through its influence over cell function. The predominant molecular transducers of force are integrins, which are a family of glycoproteins that act as extracellular matrix receptors. Integrins play an essential role in the signaling and structure of a cell and interacts with the cytoskeleton through focal adhesion proteins, which regulate cell survival, differentiation, migration, and mechanotransduction pathways [45]. Kim et al. [37] demonstrated that magnetic nanoparticles incremented the expression of β1-integrin which might led to neurite outgrowth and are involved in cellular response to mechanical forces. In addition, magnetic beads coated with β1-integrin ligand showed force-dependent focal adhesion formation, indicating that integrins can transfer external force through the plasma membrane [41].

We have demonstrated that PEI-MNPs can both penetrate inside PC12 cells through an endocytic-like mechanism and also remain attached to the cell membrane. These results led us to conclude that the uptake of PEI-MNPs by neural cells may increment the expression of integrins that favor the formation of focal adhesion proteins in the direction of the applied magnetic field resulting in the formation of neurites in this direction.

To sum up, our results have shown that PC12 neural cells with incorporated PEI-MNPs can preferentially direct the growth of neurites along the direction of an externally applied magnetic field. Moreover, in this process both the cell morphology and the number of the neurites are modified. The mechanism underlaying this neurite orientation has been demonstrated to depend on the magnetic forces acting on the MNP-bound neurites. Our findings have established the proof of concept that MNPs can be employed as enhancers of nerve regeneration under the effect of externally applied

magnetic fields. This could be the first stage for a non-invasive strategy of neural regeneration based on nanotechnological devices.

VI. CONCLUSIONS AND FUTURE PERSPECTIVES

Nerve regeneration is a major issue in the treatment of traumatic nerve injuries and has stimulated considerable bioengineering research aimed at exploring innovative strategies for physical or chemical guidance of axonal re-growth across the nerve lesion. The project outlined in this work proposes a novel minimally invasive approach for physical guidance based on synergistic use of magnetic nanoparticles (MNPs) and magnetic fields (H).

In this study, we attempted to determine whether the application of a magnetic field can affect neuron-like cells (PC12 cell line) previously incubated with polyethyleneimine-coated nanoparticles (PEI-MNPs). The selected PEI-MNPs were suitable for this purpose because they possess high saturation magnetization, negligible cytotoxicity and high capability to magnetize mammalian cells. The intracellular distribution of the PEI-MNPs analyzed at the single-cell level by dual-beam (FIB/SEM) technique revealed the coexistence of clusters of PEI-MNPs attached to the membrane and crossing the cell membrane as well as in the intracellular part of the PC12 cells.

MNPs were used to generate tensile forces under the effect of an external magnetic field and to manipulate axons in order to stimulate neurite initiation or axon elongation in the desired direction. When PC12 cells were cultured with the PEI-MNPs and exposed to an external magnetic field, particles were found in the cell body but also in the growth cone of developing neurites. In this neuron-like cell line, it was confirmed that PEI-MNPs direct the neurite outgrowth preferentially along the direction imposed by an external magnetic field.

The PEI-MNPs also affected the neurite length and cell morphology. Longer average of neurite length was found in cells loaded with PEI-MNPs.

In summary, these results showed that the use of MNPs and magnetic forces seems to be a good and novel strategy for neural manipulation.

VII. REFERENCES

1. Jain, K.K., *Advances in the field of nanooncology.* Bmc Medicines, 2010. **8**.

2. Gupta, A.K.a.G., M., *Synthesis and surface engineering of iron oxide nanoparticles for biomedical applications.* Biomaterials, 2005. **26**(18): p. 3995-4012.

3. Oh, J.K.a.P., J.M *Iron oxide-based superparamagnetic polymeric nanomaterials: design, preparation, and biomedical application.* Progress in Polymer Science, 2011. **36**(1): p. 168-189.

4. Indira, T.K.a.L., P.K., *Nanoparticles- A Review.* International Journal of Pharmaceutical Sciences and Nanotechnology, 2010. **3**(3): p. 8.

5. Tartaj, P., Morales, M., Veintemillas-Verdaguer, S., González-Carreño, T. and Serna, C.J., *The preparation of magnetic nanoparticles for applications in biomedicine.* Journal of Physics D-Applied Physics, 2003. **36**(13): p. R182-R197.

6. González-Fernández, M.A., Torres, T., Andres-Verges, M., Costo, R., de la Presa, P., Serna, C.J., Morales, M.P., Marquina, C., Ibarra, M.R. and Goya, G.F., *Magnetic nanoparticles for power absorption: Optimizing size, shape and magnetic properties.* Journal of solid State Chemistry, 2009. **182**(10): p. 2779-2784.

7. Verges, M.A., Costo, R., Roca, A.G., Marco, J.F., Goya, G.F., Serna, C.J. and Morales, M.P., *Uniform and wáter stable magnetite nanoparticles with diameters around the monodomain-multidomain limit.* Journal of Physics D-Applied Physics, 2008. **41**(13).

8. Marcos-Campos, I., Asín, L., Torres, T.E., Marquina, C., Tres, A., Ibarra, M.R. and Goya, G.F., *Cell death induced by the application of alternating magnetic fields to nanoparticle-loaded dendritic cells.* Nanotechnology, 2011. **22**(20): p. 13.

9. Laurent, S., Forge, D., Port, M., Roch, A., Robic, C., Elst, L.V. and Muller R.N., *Magnetic iron oxide nanoparticles: Synthesis, stabilization, vectorization, physicochemical characterizations, and biological applications.* Chemical Reviews, 2008. **108**(6): p. 2064-2110.

10. Mizutani, N., Iwasaki, T., Watano, S., Yanagida, T. and Kawai, T., *Size control of magetite nanoparticles in hydrothermal synthesis by coexistence of lactate and sulfate ions.* Current Applied Physics, 2010. **10**: p. 801-806.

11. Mykhaylyk, O., Almstätter, I., Sanchez-Antequera, Y., Brandt, S., Anton, M., Döblinger, D.E.M, Settles, M., Braren R., Lerche, D., Plank, C., *Silica-Iron oxide magnetic nanoparticles modified for gene delivery: a search for optimum and quantitative criteria.* Phasmaceutical Res, 2012. **29**: p. 1344-1365.

12. Ijima, M., Nomura, Y., Kamiya, H., *Effect of structure of cationic dispersants on stability of carbon black nanoparticles and further processability through layer-by-layer surface modification.* Chem. Eng. Sci., 2013. **85**: p. 30-37.

13. Kievit, F.M., Veiseh, O.,Bhattarai, N., Fang, C.,Gunn, J.W., Lee, D., Ellenbogen, L.G., Olson, J.M. and Zhang, M., *PEI-PEG-Chitosan copolymer coated iron oxide nanoparticles for safe gene delivery: synthesis, complexation, and transfection.* Adv Funct Mater, 2009. **19**(14): p. 2244-2251.

14. Calatayud, M.P., Riggio, C., Raffa, V., Sanz, B., Torres, T.E., Ibarra, M. R., Hoskins, C., Cuschieri, A., Wang, L.Y., Pinkernelle, J., Goya, G. F. , *Neuronal cells loaded with PEI-coated Fe3O4 nanoparticles for magnetically-guided nerve regeneration.* Journal of Materials Chemistry B, 2013. **1**(29): p. 3607-3616.

15. Goya, G.F., Grazú, V. and Ibarra, M.R. , *Magnetic nanoparticles for cancer therapy.* Current Nanoscience, 2008. **4**: p. 1-16.

16. Moon, T.S., *Domain states in fine particle magnetite and titanomagnetite.* Journal of Geophysical Research-solid Earth and Planets, 1991. **96**(B6): p. 9909-9923.

17. Silva, G.A., *Neuroscience technology: progress, opportunities and challenges.* Nature Review Neuroscience, 2006. **7**(1): p. 65-74.

18. Urenjak, J., Williams, S.R., Gadian, D.G., Noble, M., *Proton nuclear magnetic resonance spectroscopy unambiguously identifies different neural cell types.* J Neurosci, 1993. **13**(3): p. 981-989.

19. Blackman, C.F., Benane, S.G., House, D.E., *Evidence for direct effect of magnetic fields on neurite outgrowth.* FASEB J, 1993. **7**(9): p. 801-806.

20. Ciofani, G., Raffa, V., Menciassi, A., Cuschieri, A., Micera, S. , *Magnetic alginate microspheres: system for the position controlled delivery of nerve growth factor.* Biomed Microdevices, 2009. **11**(2): p. 517-527.

21. Kim, D.H.a.M., D.C., *Sustained release of dexamethasone from hydrophilic matrices using PLGA nanoparticles for neural drug delivery.* Biomaterials, 2006. **27**(15): p. 3031-3037.

22. Das, M., Patil, S., Bhargava, N., Kang, J.F., Riedel, L.M., Seal, S., et al, *Auto-catalytic ceria nanoparticles offer neuroprotection to adult rat spinal cord neurons.* Biomaterials, 2007. **28**(10): p. 1918-1925.

23. Saxena, S., Caroni, P., *of axon degeneration: from development to disease.* Prog Neurobiol, 2007. **83**(3): p. 174-191.

24. Griffin, J.W., Thompson, W.J., *Biology and pathology of non myelinating Schwann cells.* Glia, 2008. **56**(14): p. 1518-1531.

25. Stoll G, M.H., *Nerve injury, axonal degeneration and neural regeneration: basic insights.* Brain Pathol, 1999. **9**(2): p. 313-325.

26. Snider, W.D. and E.M. Johnson, *Neurotrophic molecules.* Annals of Neurology, 1989. **26**(4): p. 489-506.

27. Heumann, R., Korsching, S., Bandtlow, C. and Thoenen, J., *Changes of nerve growth factor synthesis in nonneuronal cells in response to sciatic nerve transection.* J. Cell. Biol., 1987. **104**: p. 1623-1631.

28. Murakami, Y., Furukawa, S., Nitta, A. and Furukawa, Y., *Accumulation of nerve growth actor protein at both rostral and caudal stumps in the transected rat spinal cord.* J Nurol Sci., 2002. **198**(1-2): p. 63-69.

29. Madduri, S., Di Summa, P., Papaloïzos, M., Kalbermatten, D. and Gander, B., *Effect of controlled co-delivery of synergistic neurotrophic factors on early nerve regeneration.* Biomaterials, 2010. **31**: p. 8402-8409.

30. Bernhardt, R.R., *Cellular and molecular bases of axonal pathfinding during embryogenesis of the fish central nervous system.* J Neurobiol, 1999. **38**(1): p. 137-160.

31. Becker, C.G., Becker, T., *Growth and path finding of regenerating axons in the optic projection of adult fish.* J Neurosci Res, 2007. **85**(12): p. 2793-2799.

32. Wen, Z., Zheng, J.O. , *Directional guidance of nerve growth cones.* Curr Opin Neurobiol, 2006. **16**(1): p. 52-58.

33. Huang, C., Borchers, C.H., Schaller, M.D., Jacobson, K., *Phosphorylation of paxillin by p38 MAPK is involved in the neurite extension of PC-12 cells.* J Cell Biol, 2004. **164**: p. 593-602.

34. Woo, S., Gomez, T.M., *Rac1 and RhoA promote neurite outgrowth through formation and stabilization of growth cone point contacts.* J Neurosci, 2006. **26**: p. 1418-1428.

35. Hynes, R.O., *Integrins: Versatility, modulation and signaling in cell adhesion.* Cell, 1992. **69**: p. 11-25.

36. Dalby, M.J., *Topographically induced direct cell mechanotransduction.* Med Eng Phys, 2005. **27**: p. 730-742.

37. Kim, J.A., Lee, N., Kim, B.H., Rhee, W.J., Yoon, S., Hyeon, T., Park, T.H., *Enhancement of neurite outgrowth in PC12 cells by iron oxide nanoparticles.* . Biomaterials, 2011. **31**(11): p. 2871-2877.

38. Pal, A., Singh, A., Nag, T.C., Chattopadhyay, P., Mathur, R., Jain, S., *Iron oxide nanoparticles and magnetic field exposure promote functional recovery by attenuating free radical-induced damage in rats with spinal cord transection.* International Journal of Nanomedicine, 2013. **2013**(8): p. 2259-2272.

39. Riggio, C., Calatayud, M.P., Sanz, B., Torres, T.E., Giannaccini, M., Ibarra, M.R., Dente, L., Goya, G.F., Cuschieri, A. and Raffa, V., *The growth of neuronal processes can be directed via magnetic nanoparticles and magnetic fields.* ACS Nano Submitted, 2013.

40. Wu, J., Pajoohesh-Ganji, A., Stoica, B.A., et al, *Expression of cell cycle proteins contributes to astroglial scar formation and chronic inflammation after rat spinal cord contusion.* J Neuroinflammation, 2012. **9**: p. 169.

41. Katsumi, A., Naoe, T., Matsushita, T., Kaibuchi, K., Schwartz, M.A., *Integrin activation and matrix binding mediate cellular responses to mechanical stretch.* J Biol Chem, 2005. **280**: p. 16546-16549.

42. Ali, M.H.a.S., P.T., *Endothelial responses to mechanical stress: where is the mechanosensor?* Crit Care Med, 2002. **30**(5 Suppl): p. S198-206.

43. Kumamoto, C.A., *Molecular mechanisms of mechano sensing ank their roles in fungal contact sensing.* Nat Rev Microbiol, 2008. **6**(9): p. 667-673.

44. Makino, A., Prossnitz, E.R., Bunemann, M., Wang, J.M., Yao, W., Schmid-Schonbein, G.W., *G protein coupled receptors serve as mechanosensors for fluid shear stress in neutrophils.* Am J Physiol Cell Physiol, 2006. **209**(6): p. C1633-1639.

45. Chiquet, M., Gelman, L., Lutz, R., Maier, S., *From mechanotransduction to extracellular matrix gene expression in fibroblasts.* Biochim Biophys Acta, 2009. **1793**(5): p. 911-920.

46. Kim, S., Im, W-S., Kang, L., Lee, S-T., Chu, K., Kim, B.I. , *The application of magnets directs the orientation of neurite outgrowth in cultured human neuronal cells.* Journal of Neuroscience Methods 2008. **174**: p. 91-96.

47. Sugimoto, T., Matijevic, E., *Formation of uniform spherical magnetite particles by crystallization from ferrous hydroxide gels.* J. Colloid Interface Sci, 1980. **74**(1): p. 227-243.

48. Goya, G.F., Berguo, T.S., Fonseca, F.C. and Morales, M.P., *Static and dynamic magnetic properties of spherical magnetite nanoparticles.* Journal of Applied Physics, 2003. **94**(5): p. 3520-3528.

49. Riggio, C., Calatayud, M.P., Hoskins, C., et al, *Poly-L-lysine coated magnetic nanoparticles as intracellular actuators for neural guidance.* Int j Nanomedicine, 2012. **7**: p. 3155-3166.

50. Soenen, S.J.H., Nuytten, N., De Meyer, S.F., De Smedt, S.C. and De Cuyper, M. , *High intracellular iron oxide nanoparticle concentrations affect cellular cytoskeleton and focal adhesion kinase-mediated signaling.* Small, 2010. **6**: p. 832-842.

51. Babic, M., Horák, D., Trchová, M., Jendelová, P., Glogarová, K., Lesný, P., Herynek, V., Hájek, M. and Syková, E., *Poly (L-lysine) - modified iron oxide nanoparticles for stem cell labeling.* Bioconjugate Chemistry, 2008. **19**: p. 740-750.

52. Hong, J.H., Noh, K.M., Yoo, Y.E., Choi, S.Y., Park, S.Y., Kim, Y.H. and Chung, J.M., *Iron promotes the survival and neurite extension of serum-starved PC12 cells in the presence of NGF by enhancing cell attachment.* Mol Cells, 2003. **15**(1): p. 10-19.

53. Yoo, Y.E., Hong, J.H., Hur, K.C., Oh, E.S. and Chung, J.M., *Iron enhances NGF-induced neurite outgrowth in PC12 cells.* Mol Cells, 2004. **17**(2): p. 340-346.

54. Pisanic, T.R., Blackwell, J.D., Shubayev, V.I., Fiñones, R.R. and Jin, S., *Nanotoxicity of iron oxide nanoparticle internalization in growing neurons.* Biomaterials, 2007. **28**: p. 2572-2581.

VIII. ANNEX

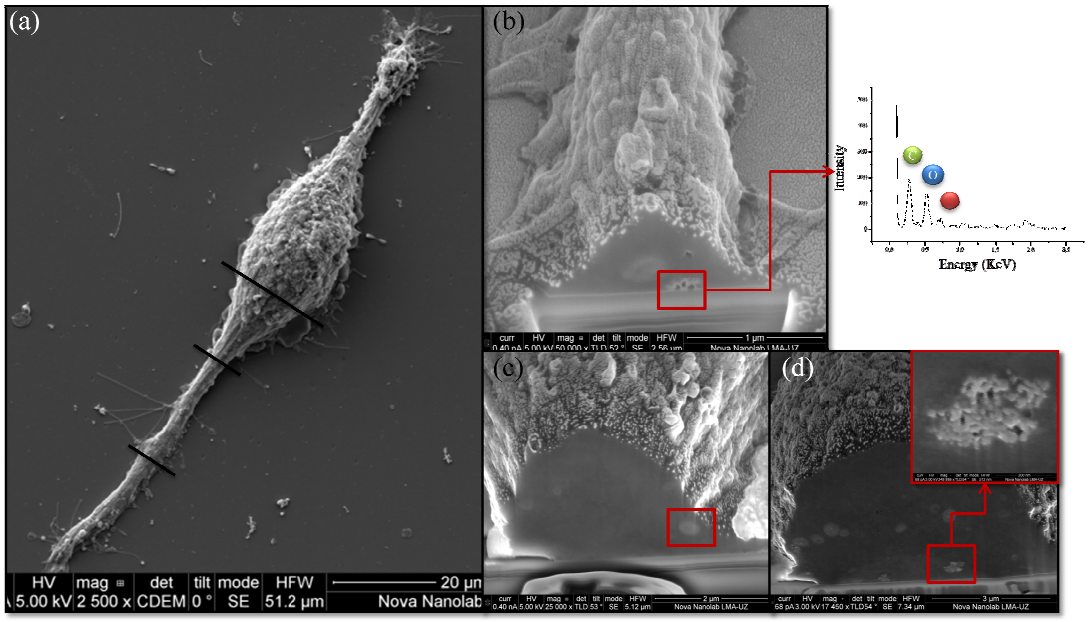

Figure A1. SEM images of PC12 cells ($MNP^{+}H^{+}$) cross-sectioned by FIB after 24 hours incubation at 10 µg/mL of PEI-MNPs and for 4 days of differentiation. *(a) The whole cell previously to be cross-sectioned. (b) And (c) Intracellular space of the axon in where we could observe the presence of PEI-MNPs agglomerates in both attach to the membrane and inside the axon. The inset corresponds with the EDX spectra of the highlight part. (d) Neural soma intracellular space in where we could see the presence of PEI-MNPs. The inset shows a detail of the PEI-MNPs inside the soma.*

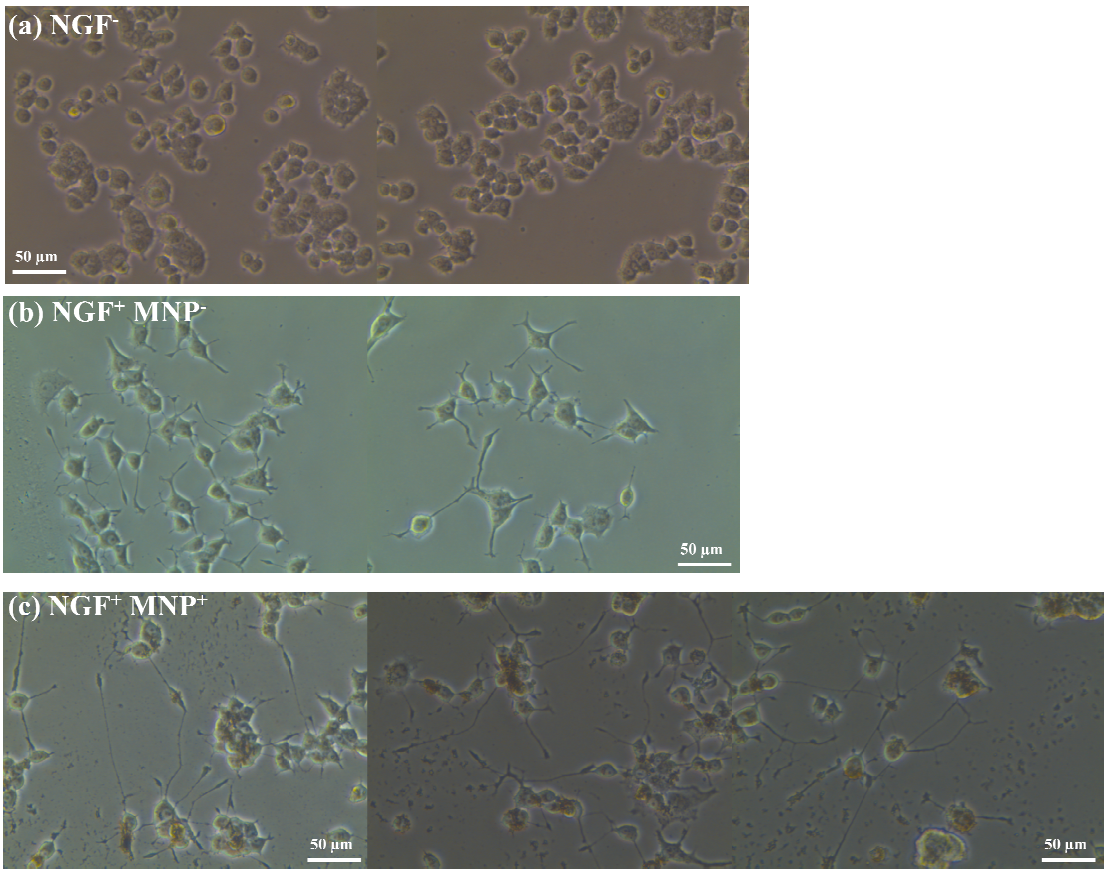

***Figure A2. Phase contrast images of PC12 cells**: (a) undifferentiated, (b) with NGF (NGF^+, MNP^-), (c) with NGF and PEI-MNPs (NGF^+, $PEI\text{-}MNPs^+$). The b and c images were recorded the 4^{th} day of inducing differentiation. These results indicate that PEI-MNPs promoted neurite outgrowth relative to non-treated cells.*

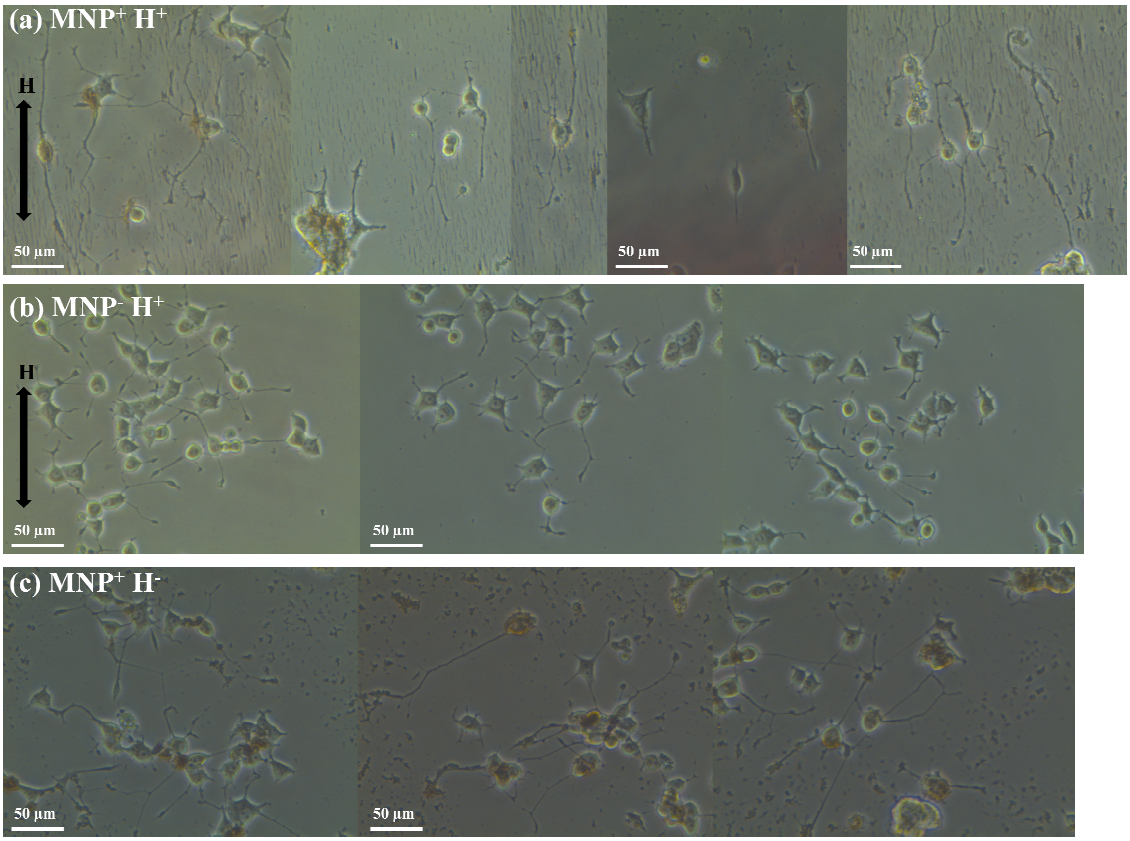

***Figure A3. Phase contrast images of PC12 cells**: (a) incubated with PEI-MNPs and differentiated in the presence of a magnetic field (MNP^+ H^+), (b) differentiated in the presence of a magnetic field without PEI-MNPs (MNP^- H^+) and, (c) incubated with PEI-MNPs in the absence of an external magnetic field (MNP^+ H^-). The results indicated that in presence of both particles and magnetic field, neurites preferentially grow during the neural processes in the direction imposed by the external magnetic field.*

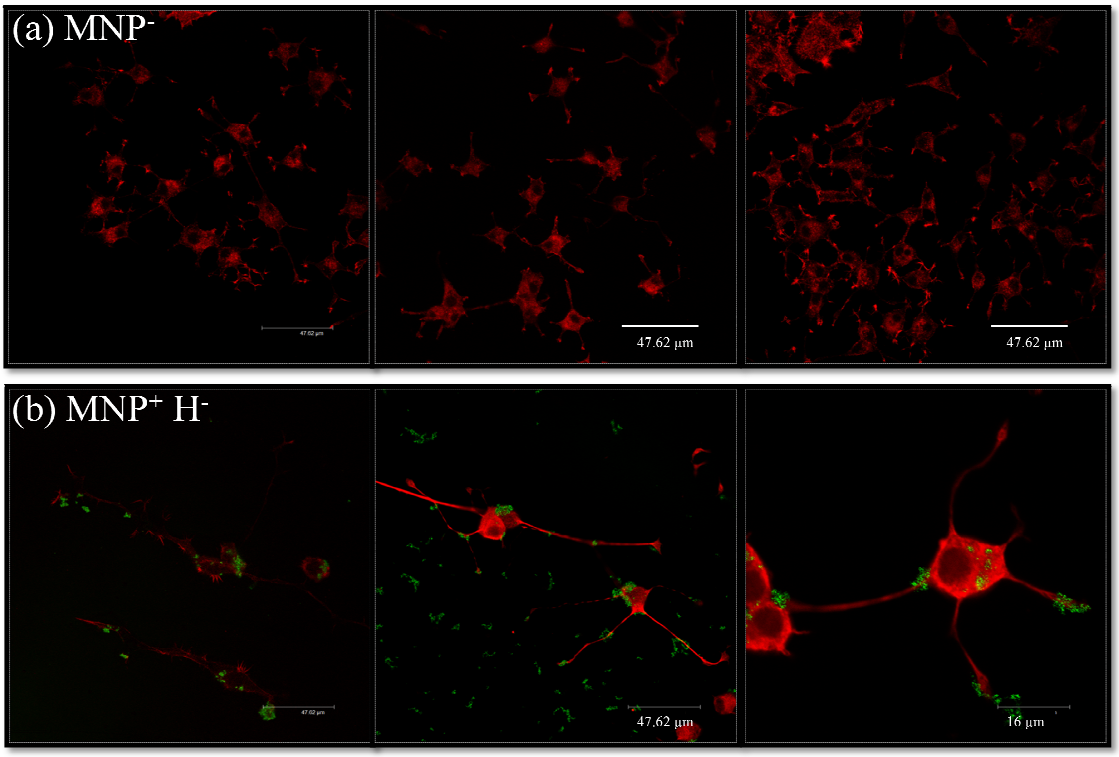

Figure A4. Immunofluorescence images of differentiated PC12 cells 4 days control (a) and after treatment with f-PEI-MNPs (b). *Red fluorescence represents actin microfilaments (a) or microtubules (b) and green color represents nanoparticle reflection. (a) Examples of PC12 cells without MNPs treatment; it can be seen that PC12 cell exhibited spherical unpolarized shaped with short neurites. (b) PC12 cells treated with MNPs; cells exhibited typically neuron shape with a long slender axon and several shorter dendrites.*

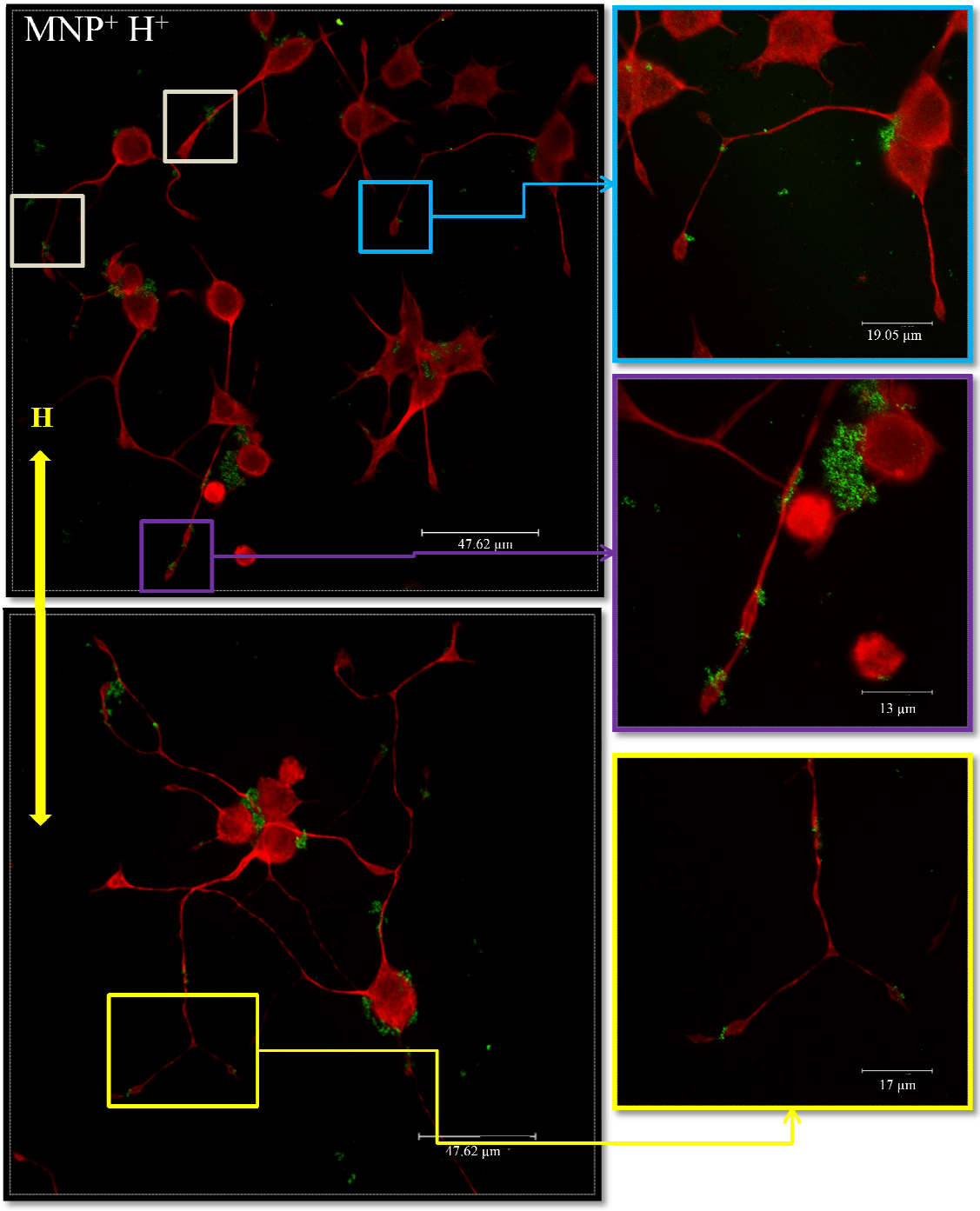

Figure A5. Immunofluorescence images of differentiated PC12 cells 4 days after treatment with f-PEI-MNPs in the presence of magnetic field (MNP$^+$ H$^+$). *Red fluorescence represents tubulin microtubules and green color represents nanoparticle reflection and yellow line represents the magnetic field direction. (a) And (b) MNP$^+$ H$^+$ PC12 cells stained with anti-tubulin III antibodies. The inset images represent the detail of axon of the PC12 cells in which it is observed the PEI-MNPs inside the axon.*